TECHNISCHE UNIVERSITÄT MÜNCHEN

Fakultät für Medizin

Klinikum rechts der Isar

Experimentelle Anästhesie

The effect of isoflurane and xenon on the synapse elimination by astrocytes in the absent/present of $A\beta_{1-42}$

Dai Shi

Vollständiger Abdruck der von der Fakultät für Medizin der Technischen Universität München zur Erlangung des akademischen Grades eines

Doktors der Medizin （Dr. med.）

genehmigten Dissertation.

Vorsitzender: Prof. Dr. Ernst J. Rummeny

Prüfende/r der Dissertation:

1. apl. Prof. Dr. Gerhard Rammes
2. Priv.-Doz. Dr. Frauke Neff

Die Dissertation wurde am 18.07.2019 bei der Technischen Universität München eingereicht und durch die Fakultät für Medizin am 11.02.2020 angenommen.

Abstract:

Background: Synaptic pruning, a process of synapse elimination, may be aberrantly activated in the aged brain and contribute to synapse loss and hence cognitive impairment in Alzheimer's disease (AD). Postoperative cognitive dysfunction (POCD) has been reported to be related to AD. It has been hypothesised that POCD and AD may be triggered by perioperative factors such as anaesthesia. Multiple epidermal growth factor (EGF)-like domains 10 (MEGF10) is one of the phagocytic proteins which helps the elimination of inactive synapses by astrocytes. β-amyloid peptide 1-42 ($A\beta_{1-42}$) is a major endogenous pathogen underlying the aetiology of AD. However, it is still unclear how anaesthetics and $A\beta_{1-42}$ affect MEGF10 function and hence synaptic pruning. The present study intends to elucidate the interactions of isoflurane (370μM), xenon (1.9mM) and $A\beta_{1-42}$ with MEGF10-dependent synapse elimination which may have implication for POCD and AD.

Methods: Brain slices of wild type and adeno-associated virus (AAV)-induced MEGF10 knock-down mice were used. Murine cultured astrocytes and hippocampal brain slices were treated with either isoflurane (90mins) or xenon (60mins) or in combination with $A\beta_{1-42}$ (90min). By means of immunofluorescence and western blot techniques MEGF10 expression, dendritic spine density (DSD) and co-localisation of pre- (synaptophysin) and postsynaptic (PSD95) associated sites in GFAP stained astrocytes were quantified.

Results: Isoflurane and xenon reversible decreased DSD in brain slices and reduced MEGF10 expression in cultured astrocytes. Neither isoflurane nor xenon changed the amount of pre- and postsynaptic material inside astrocytes, whereas $A\beta_{1-42}$ elevated these pre- and postsynaptic markers and decreased DSD. The combined application with either isoflurane or xenon reversed these effects. AAV-induced knock-down of MEGF10 reduced synaptophysin and PSD95 inside astrocytes, indicating the involvement of MEGF10 in synaptic elimination. Interestingly, in the presence of $A\beta_{1-42}$ both anaesthetics decreased MEGF10 expression in astrocytes.

Conclusion: The presented data suggests that the decrease of DSD caused by isoflurane and xenon is not due to synaptic elimination mediated by the MEGF10 pathway. Isoflurane and xenon are able to reverse the $A\beta_{1-42}$-induced elevation of synaptic elimination presumably through MEGF10 downregulation, which suggests an astrocytic-dependent elimination of synapses via the MEGF10 signalling pathway. In conclusion, this in vitro study revealed that anaesthetics reversible interfere with spine dynamics but rather reverse the synaptotoxic effects of $A\beta_{1-42}$ on the dynamic properties of synapses. These results suggest only a minor role of anaesthetics in triggering and acceleration of POCD and Aβ-derived pathophysiology in AD.

Zusammenfassung

Hintergrund: Synaptische Eliminierung, kann im älteren Gehirn auf verschiedene Weise aktiviert werden und zum Verlust von Synapsen und somit zur kognitiven Beeinträchtigung ähnlich wie bei der Alzheimer-Krankheit (AD) beitragen. Es wurde berichtet, dass postoperative kognitive Dysfunktion (POCD) mit AD zusammenhängt. Es wird diskutiert, ob POCD und AD durch perioperative Faktoren wie Anästhesie ausgelöst werden können. Multiple Epidermal Growth Factor (EGF)-ähnliche Domänen 10 (MEGF10) ist eines der Phagozytenproteine, dass die Beseitigung inaktiver Synapsen durch Astrozyten unterstützt. Das β-Amyloidpeptid 1-42 ($A\beta_{1-42}$) ist ein charakteristisches endogenes Pathogen, der die Ätiologie von AD zugrunde liegt. Es ist jedoch immer noch unklar, wie Anästhetika und $A\beta_{1-42}$ die MEGF10-Funktion und damit die synaptische Eliminierung beeinflussen. Die vorliegende Studie beabsichtigt, die Wechselwirkungen von Isofluran (370 uM), Xenon (1,9 mM) und $A\beta_{1-42}$ mit der MEGF10-abhängigen Elimination von Synapsen aufzuklären, welche auch Auswirkungen auf POCD und AD besitzen kann.

Methoden: Astrozytäre Kulturen und hippokampale Hirnschnitte wurden entweder mit Isofluran (90 Minuten), Xenon (60 Minuten) oder $A\beta_{1-42}$ (90 Minuten) oder in Kombination behandelt. Untersucht wurde die MEGF10-Expression und die Dichte der dendritischen Dornfortsätze (DSD) in hippokampalen Neuronen. In Hippokampus von Wildtyp- und Adeno-associated virus (AAV)-induzierten MEGF10-Knockdown-

Mäusen wird die Ko-lokalisation von astrozytären Markern (GFAP) und Markern der Prä- (Synaptophysin) und Postsynapse (PSD95) mittels Immunfluoreszenzverfahren quantifiziert.

Ergebnisse: Sowohl Isofluran als auch Xenon verminderten reversibel die DSD und reduzierten gleichzeitig die Expression von MEGF10. Isofluran und Xenon veränderten nicht die Menge an Synaptophysin und PSD95 in den Astrozyten. $A\beta_{1-42}$ hingegen erhöhte die Ko-lokalisation von prä- und postsynaptischen Markern in den Astrozyten und verringerte auch die DSD. Die kombinierte Anwendung mit Isofluran oder Xenon reversierte diese Effekte. Der MEGF10 knock-down reduzierte prä- und postsynaptisches Material in den Astrozyten und deuted auf die Beteiligung von MEGF10 an der synaptischen Eliminierung hin. Interessanterweise verringerten beide Anästhetika in Gegenwart von $A\beta_{1-42}$ die MEGF10-Expression in Astrozyten.

Schlussfolgerung: Die vorgelegten Daten legen nahe, dass die durch Isofluran und Xenon verursachte Abnahme der DSD nicht auf eine synaptische Eliminierung durch den MEGF10-Signalweg zurückzuführen ist. Da Isofluran und Xenon, vermutlich durch eine MEGF10-Herabregulierung, die durch $A\beta_{1-42}$ induzierte verstärkte Eliminierung von Synapsen reversiert, kann vermutet werden, dass dies über einen Astrozyten abhängigen MEGF10-Signalweg erfolgt. Zusammenfassend konnten wir eine Wechselwirkung von Isofluran, Xenon und $A\beta_{1-42}$ auf die dynamischen

Eigenschaften von Synapsen zeigen. Dabei wurde deutlich, dass Anästhetika einer $A\beta_{1-42}$ vermittelten Synaptotoxizität eher entgegenwirken. Diese Ergebnisse können helfen, den Mechanismus der AD-Progression zu verstehen und eine mögliche Interaktion von Anästhetika mit der AD Pathophysiologie zu klären.

Agenda

I Introduction

1.1 Alzheimer's disease

40 million people in the world are suffering from Alzheimer's dementia, and the number will grow to 160 million by this mid-century, according to the annual report of the Alzheimer's Association[1]. Alzheimer's disease (AD) is the most common cause of dementia in elder adults[1], characterized as progressive wide range cognitive decline. The AD patients may have difficulties with memory, orientation, language and problem-solving, affecting their daily activities[2]. The two key hallmarks of AD are extracellular beta-amyloid (Aβ) (plaques) and intracellular twisted strands of the protein tau (tangles)[3].

According to age, AD could be classified as two subtypes: 1) early-onset AD (EOAD)(Individuals develop Alzheimer's symptoms before age 65, or even as early as age 30); 2) late-onset AD (LOAD)(individuals develop AD at age 65 or later)[1]. In addition, AD could also be divided into three different types according to family history: 1) autosomal dominant AD (ADAD) (<5% of all cases); 2) familial AD (15-25% of all cases); 3) sporadic AD (sAD) (75% of all cases) [4].

The diagnosis of AD is based on core clinical criteria, which includes the reports from the patient or family members, the symptom progression, cognitive tests, and general neurological judgment[5]. Because the diagnosis of AD should exclude the other causes of cognitive decline, the testing of the biomarkers of AD could increase the

certainty that the clinical dementia syndrome refers to the AD pathophysiological process[6]. Except for Aβ plaques and protein tau tangles, low CSF Aβ, elevated CSF-tau can also be assessed[7, 8]. However, due to the high costs of the biomarker testing and the lack of treatment means, the diagnosis of AD in the clinic still relies on the neuropsychological testing[5, 6].

The therapy of AD has not made great progress since this disease was detected 100 years ago. The cause of AD has not been fully understood, and the pathogenesis of dementia is multifactorial[3]. For years, researchers have focused on the intracellular tangles and extracellular plaques. The intracellular tangles are formed from the microtubule-associated protein Tau in the neurons[9]. The amyloid plaques, which were supposed to block the connections of the neuron and cause the death of the cells, are insoluble deposits in the brain[3]. The plaques are formed by the small soluble Aβ-oligomers generated through enzymatic cleavage of the transmembrane amyloid precursor protein (APP)[10, 11]. A growing number of existing studies have reviewed that the soluble form of Aβ is more toxic to neurons rather the extracellular plaques, and it can induce more synapse loss[10, 12-15].

1.2 $A\beta_{1-42}$

Although it is the subunit of Abeta fibrils, Aβ is a normal outcome of the metabolism of APP. It is generated through enzymatic cleavage of APP by β-secretase

in the extracellular and γ-secretase protease complex in the middle of the membrane. The formation of Aβ from APP is presented as follows (Fig 1)[16].

However, the mutations in APP and in the γ-secretase protease complex can help generate Aβ and thus lead to the increase in Aβ in the brain[13, 17]. The most common Aβ peptide is 40-42 amino acids length.[13]

Recently, numerous studies have reported that soluble Aβ-oligomers were more toxic to neurons and could induce more synapse loss than the extracellular plaques [10, 12-15]. Previous studies revealed that the synapse loss might lay the physical basis for dementia in AD [18-20 21].

Fig 1 Aβ formed from APP (Spies, P. E. et al. 2012 Reviewing reasons for the decreased CSF Abeta concentration in Alzheimer disease)

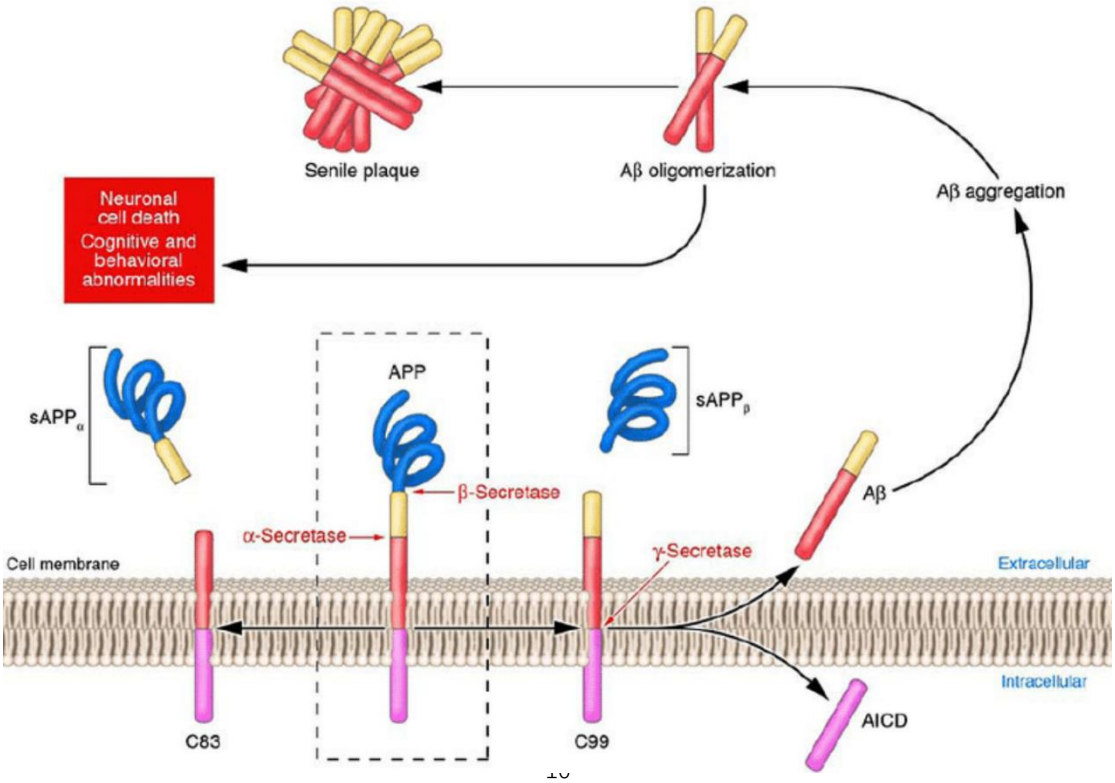

Previous study revealed that using the pharmacological antagonists of Aβ oligomers to reduce the binding of Aβ oligomers to neurons could mitigate spine loss in neurons and ameliorate cognitive deficit[22]. Accordingly, the research of the association between $A\beta_{1-42}$ and synapses loss could be one aspect to investigate the mechanism of AD pathogenesis.

1.3 Synapses and dendritic spines

Synapses, in which our memory traces are encoded and stored[23], always act as an attractive target to study cognitive disorders. Synapses can be classified as 1) active synapses which are fully assembled in the post-synaptic membrane with AMPA-type glutamate receptors and can be physiological active after getting the input from the active pre-synaptic element; and 2) silent synapses. In contrast, the silent synapses have no AMPA-type glutamate receptors but NMDA receptors in the post-synaptic membrane; they are inactive under regular synaptic transmission[24, 25]. Silent synapses are the cellular phenomenon of the brain potential and could be activated by inserting AMPA-type receptors into the postsynaptic membrane[26, 27].

Synapse (including the silent one) re-modelling takes places in the brain during the procession of memory and cognition [28]. Besides, synaptic loss is well established as a major structure disorder in the cognitive decline of AD[19]. One previous study revealed

that synapse loss was associated with small soluble Aβ-oligomers at the early stage of AD[29].

Dendritic spines are highly dynamic neuronal protrusion, acting as the postsynaptic element of excitatory synapses[30]. There are 5 different shapes of spines, including: filopodium, thin, stubby, mushroom and cup shaped[30]. Spine morphology, formation, and clearance can be modulated in the brain by input from the environment, which is crucial for the changes of memory and cognition in the brain [31]. Spine dynamics are cellular phenomena for cognition and memory[31]. Several previous studies have demonstrated that dendritic spine density could decrease in AD[21, 32].

1.4 Hippocampus, dentate gyrus and Alzheimer's disease

The hippocampus is a small region of the brain, locating beside the middle line of the brain and embedded into the temporal lobe[33]. The basic hippocampal circuit starts at the dentate gyrus (DG) region, next comes to the CA4, and then the small regions called CA3, CA2 and CA1, respectively. After CA1 the circuit projects to the subiculum. Researchers always defined the four CA regions as "hippocampus proper". The functional and structure changes in hippocampus, including synaptic remodeling, long-term potentiation (LTP) and long-term depression (LTD), are crucial for the memory formation and studying[34]. Given that the major functions of hippocampus are

learning and memory, this small region has been well studied in the field of Alzheimer' disease and other cognitive disorders, and the atrophy of hippocampus is considered a hallmark of neurodegeneration. Several studies reported the synapse loss in hippocampus in early Alzheimer's disease[35-37]. It has also been reflected a significant loss of neurons in cortex, and these neurons allow for a direct projection to the hippocampal dentate gyrus.

Dentate gyrus, as the beginning of the hippocampal circuit, is considered to be vital for associative memory[38]. Previous studies reported that there was a 35-44% reduction of spine numbers and a 60% reduction of spine density in the dentate gyrus in AD[39, 40]. In the early stage of AD, the loss of neuro-connectivity in dentate gyrus was considered to improve the memory decline[41].

1.5 MEGF10

Astrocytes, as the type of numerous cells in the brain, are known as the structure and trophic supporter of the neuron, the neuron and synapses functions elevator[42-44], and as a scavenger of CNS [45]. Astrocytes could help eliminate synapses via the MEGF10 pathway. Without MEGF10, astrocytes displayed about 50% reduction in the relative engulfment ability[46].

Multiple EGF-like domains 10 (MEGF10) is a mammalian ortholog of *drosophila draper*[47, 48] and *c elegans* CED-1[49]. A transmembrane protein acts as one phagocytic

receptor existing on the surface of the phagocytic cells and recognizes the “Eat me signal”[50]. Studies revealed that MEGF10 acts as a receptor of C1Q expressed on the apoptotic cells and silent synapses[50-52]. Since the silent synapse can be fully assembled into the active one, synapse loss can be the consequence of the elevated expression of MEGF10 on the astrocytes. The previous study also demonstrated that MEGF10 acts as a receptor for the uptake of amyloid-β[53].

1.6 Isoflurane and xenon

Isoflurane is a widely used inhalational anesthetic in the clinic, which may bind to GABA, glutamate and glycine receptors, but has different effects on each receptor[54-57]. There is some controversy showing that isoflurane might be associated with cognitive decline in elders through accelerating the pathogenesis of AD[58, 59 60, 61]. Numerous studies established that isoflurane could interact with three amino acid residues (G29, A30, and I31) of amyloid beta peptide and trigger Aβ aggregation[62]. Thus, it raised the public concern that isoflurane may cause brain damage via accelerating the onset of Alzheimer’s disease[63].

Xenon, a colorless, odorless noble gas is a glycine-site NMDA receptor antagonist[64, 65], and can also interact with AMPA receptors as an antagonist and other ion channels, which may be complementary[66, 67]. Different from nitrous oxide, ketamine and other NMDA receptor antagonists, xenon has only neuroprotective

effects and no co-existing neurotoxic effect [68]. Previous studies reported that xenon could play a neuroprotective role when the concentration ranged from 35%-75%[69, 70]. The responsible mechanism underlying the neuroprotective effects of xenon probably lays in its NMDA receptor antagonisms, and reducing overexcitation of NMDA receptors under the excitotoxic stress conditions[70, 71]. Xenon inhibited the AMPA-and kainite induced membrane current may also be a potential mechanism[67].

Though it is very expensive, xenon has been used as a general anesthetic, which is well confirmed as a neuroprotectant [72-74]. However, there has been no evidence to show the different incidence of POCD in patients anesthetized with xenon compared with those anesthetized with any other anaesthetics. A previous study reported that xenon attenuated LTP in the hippocampus reversible[75], which might suggest a potential effect on the plasticity of synapses and cognition[76].

Since the mechanisms of isoflurane and xenon are different, and because of the different effect on the NS, those two anesthetics were taken in this study to study their effect on synapse re-modeling and the interference with $A\beta_{1-42}$.

.

1.7 Postoperative cognitive dysfunction

From 1996 to 2006, the rate of surgery performed increased by 300 percent, and the rate continues to increase annually[77]. In the meantime, the aging population are increasing rapidly. As a growing number of older patients undergo the operation, the

age-dependent perioperative disorders have raised public concern[78]. Postoperative cognitive dysfunction (POCD) is one of those disorders.

POCD is defined as cognitive decline after surgery, especially extensive surgery[79, 80]. It is primarily known as a result after cardiac surgery, and a postoperative complication of noncardiac surgery, which takes place after the surgery and always lasts for 6 months[81, 82]. The impairment includes memory decline, impairment of the ability to combine tasks, and impairment of psychomotor dexterity[79]. A previous study revealed that POCD may occur at any age but tends to have a longer and more serious consequence in patients over age 60[83]. Besides the age, the risk factors of POCD are proved as below.(table 1)[79]

Table1:

Risk factors for postoperative cognitive dysfunction (POCD)

	Risk factors
Patient	advanced age; pre-existing cerebral, cardiac, or vascular disease; preoperative mild cognitive impairment (MCI); low educational level; history of alcohol abuse
Operation	extensive surgical procedure, intra- or postoperative complications, secondary surgery
Anesthesia	long-acting anesthetic, marked disturbance of homeostasis, organ ischemia due to hypoxia and hypoperfusion, intra- or postoperative anesthesiological complications

The diagnosis of the POCD requires both pre- and postoperative psychometric testing[79]. The testing consists of the examination of functional ability in memory, attention, language, motor function and other aspects of cognition[79].

The pathogenesis of the POCD is multifactorial, and the mechanisms underlying are not yet fully clear[83]. The findings of animal experiments suggest that the immune response to surgery plays an important role in the pathogenesis of POCD[84, 85]. Surgery, anesthesia, and many perioperative factors could also be the reasons for POCD[82, 86].

Though there is no research concluded that general anaesthesia has a clear link with POCD, the shorter the treatment duration with the anaesthetic, the shorter the duration of cognitive impairment in POCD[83]. Qiao, et al. also revealed in 2015 that the inhalational anaesthesia was more likely to induce POCD in the elder patients than intravenous anaesthesia[58].

The previous study did longitudinal research on the development of POCD and course of Alzheimer's disease[87]. Its result revealed that postoperative cognitive function was seriously impaired in patients who already had a mild or subclinical cognitive impairment. The relation between POCD and Alzheimer's disease has aroused increasing concern[59, 88]. Nowadays, studies prefer the perspective that the serious and long prolonged POCD happens to elder patients who are on the early stage of Alzheimer's disease before surgery[89, 90].

1.8 Aims

This study primarily aimed to elucidate the interaction of two anaesthetics, differing in their mechanisms of action (MOA), with spine density dynamics and $A\beta_{1-42}$ – derived AD pathology. Besides, the study also focused on the association between synapses loss and the MEGF10 signaling pathway, thereby investigating possible implications for the pathogenesis of AD and POCD

Part i: Application of anesthetics to brain slices

In general, the incidence of POCD after accepting the extensive operation was lower in young adult people, who were not in the progression of AD. In the meantime, even if they had POCD, the duration of cognitive decline would be shorter than the elders[79]. Given that synapse loss is one of the potential mechanisms underlying the cognitive decline, this study was designed to explore the synapse loss of hippocampal DG region after those patients, who are not in the progression of AD, were exposed to general anesthetics.

To simulate the normal brain without $A\beta_{1-42}$ aggregation, the brain slices and in-vitro cultured astrocytes from C57/BL6 mice were used. After the brain slices and astrocytes were exposed to 370μM isoflurane or 1.9mM xenon, the dendritic spine density, the pre-and postsynaptic marker inside the astrocytes and the expression of MEGF10 on the astrocytes were tested to investigate the influence of isoflurane and xenon on the synapse loss.

Part ii: $A\beta_{1-42}$ treated brain slices receive anesthesia

The level of $A\beta_{1-42}$ peptide in the brain rises early in the progress of AD. Even when the patients are still in the stage of cognitive normal or cognitive mildly decline, there would have already been the rise in $A\beta_{1-42}$ peptide in their brain [10, 91]. Since AD is an age-dependent disease, the proportion of elderly patients is very high. Many elder patients are already on the very early stage of AD before accepting the extensive operation. Researchers hypothesized that anaesthetics could aggravate the neurotoxic effect of $A\beta_{1-42,}$ which might be the reason of cognitive decline after the extensive operation[59, 63, 92]. Thus, the higher incidence of POCD in elder patients may result from the higher concentration of $A\beta_{1-42}$ in the brain of elder patients, many of whom are on the early stage of AD.

Due to the crucial role of spine loss of the hippocampal DG region in the cognitive decline and Alzheimer's disease, the spine density and synapse elimination in DG region were taken as the key points here. It was proved that volatile anaesthetics could modulate the dendritic spine density[93, 94], and a previous study also revealed that $A\beta_{1-42}$ decreased dendritic spine density in the CA1 region[21]. However, whether isoflurane and xenon can affect the neurotoxic effect of $A\beta_{1-42,}$ and whether the interaction of isoflurane, xenon, and $A\beta_{1-42}$ can enhance or attenuate the synaptic pruning via the MEGF10 pathway have been rarely discussed.

In the present study, the neurotoxic effect of 50nM $A\beta_{1-42}$ on the spines in DG region, and the interaction of $A\beta_{1-42}$ with isoflurane (370μM) and xenon (1.9mM) were

investigated. Furthermore, this study attempted to reveal the contribution of MEGF10 in synapse elimination by quantifying dendritic spine density, astrocytic-dependent synaptic pruning, and MEGF10 expression.

II Materials and Methods

Animals:

C57BL/6 mice were obtained from the Charles River Lab (Germany). Two female C57BL/6 mice and one male C57BL/6 mice were bred for puppies. Male GFP-M(Thy1-eGFP) mice[78] were purchased from the Jackson Laboratory (USA) and were interbred with female C57BL/6 to generate. The genotyping of the new generation was performed 3 weeks postnatal, the tissues from the ears were sent to the genotyping lab of Charles river laboratory (Germany). The protocol is described below (Table 2). All the animals were bred in the mouse room of the Experimental Anesthesiology of Klinikum Rechts der Isar, TUM and under standard conditions (temperature 21 ± 1 °C, 12:12 h light/dark cycle). The condition was monitored every day. Food and water were provided ad libidum. The experiments were approved by the Ethical Committee on Animal Care and Use of the Government of Bavaria, Germany.

Table 2:

Protocol of genotyping (obtained from the neurodegenerative disease center of germany)

Mauslinie: eGFP-M

Primer:

Name	Sequence (5´-3`)	Length (bp)	Temp. (°C)
IMR 0872	AAG TTC ATC TGC ACC ACC G	19	56,7

IMR 1416	TCC TTG AAG AAG ATG GTG CG	20	57,3

PCR-kit: 25µl

Volumen (µl)	Product	Concentration
10	5Primer HotMasterMix (x2,5)	
1	IMR 0872	20 µM
1	IMR 1416	20 µM
2	Template DNA	
11,2	H_2O	

PCR-Prgramm (Eppendorf Cycler): GFP

Step	Temperatur (°C)	Time	Repeat
1	94	1´30´´	x1
2	94	30´´	x35
3	60	1´	
4	72	1´	
5	72	2´	x1
6	10	unlimited	

results: Agarosegel 1,5%

Mause	Transgen 173 bp

Positive	+
Negative	-

Brain slice preparation

After being anesthetized with isoflurane, mice (8 weeks) were killed by cervical dislocated. Brains were removed quickly from the skull and sliced sagittally (100μm) in an ice cold, carbogen (95%O2, 5%CO2) saturated cutting solution (Table 3) by using a vibratome (Leica VT 1000s, Germany). The slices were incubated in a carbogen saturated artificial cerebrospinal fluid (Table 4) at 35°C for 30min, then in the room temperature(15°C-20°C) for another 60min for recovery.

Table 3:

Cutting solution

Substance	MW	Concentration(mM)
NaCl	58.44	125
KCL	74.55	2.5
NaH2PO4-monohydrate	137.99	1.25
D-(+)Glucose-monohydrate	198.17	25
NaHCO3	84.01	25
MgCl2-Hexahydrate	203.30	6

CaCl2-Dihydrate	147.01	0.5

Table 4:

Artificial cerebrospinal fluid

Substance	MW	Concentration(mM)
NaCl	58.44	125
KCL	74.55	2.5
NaH2PO4-monohydrate	137.99	1.25
D-(+)Glucose-monohydrate	198.17	25
NaHCO3	84.01	25
MgCl2-Hexahydrate	203.30	1
CaCl2-Dihydrate	147.01	2

In vitro astrocyte culture

After being anesthetized with isoflurane, C57BL/6 mice (P0-P4) were disinfected by 70% Ethanol, then decapitated. Brains were removed from the skull quickly with the sterile tweezers and dipped in the ice-cold Hanks‘ balanced salts Buffer (HBSS, Biowest, France). Under the dissecting microscope (Leica, Germany), the cerebellum was removed, and the brain was separated into two hemispheres. The meninges were peeled, the vessels were removed carefully. The hippocampi were dissected and were

incised into 1mm pieces. The tissue pieces were digested by 0.125% trypsin (Sigma-Aldrich, USA) at 37°C at the water bath for 30min. Mixed by shaking every 10 min. After 30min, the digestion procedure was terminated by the same volume bovine serum. The mixed cell turbid liquid was centrifuged for 5 min at 300 x g (Eppendorf, Germany) to pellet the hippocampi tissue pieces. The pellet was re-suspended by HBSS and washed twice before re-suspended with 10ml culture medium (the DMEM-F12(Biowest, France) + 10% heat-inactivated fetal bovine serum (Biowest, France) + 1% Penicillin/Streptomycin (Thermo Fisher, USA)). The density of the cells was detected with the hemocytometer, the calculation has followed the protocol from the website of Abcam protocols. 200ul cell suspension was taken out and placed into a vial, added 200ul Trypan blue into the vial and mixed thoroughly. 100 µL of the mixed cell suspension was taken and applied to the glass hemocytometer (HBG, Germany), very gently filled the chamber underneath the coverslip, used the microscope, focused on the grid lines of the hemocytometer. Used a hand tally counter, counted the live, unstained cells (live cells do not take up Trypan Blue) in one set of 16 squares (Fig. 2). Counted all 4 sets of 16 corners. Took the average cell count from each of the sets of 16 corner squares. Multiplied by 10,000 (10^4) and multiplied by 2 to correct for the 1:2 dilution from the Trypan Blue addition (formula 1). The final density of the cells should be $10^5/mm^3$ by being diluted with culture medium which was described above.

Fig 2 (Abcam)

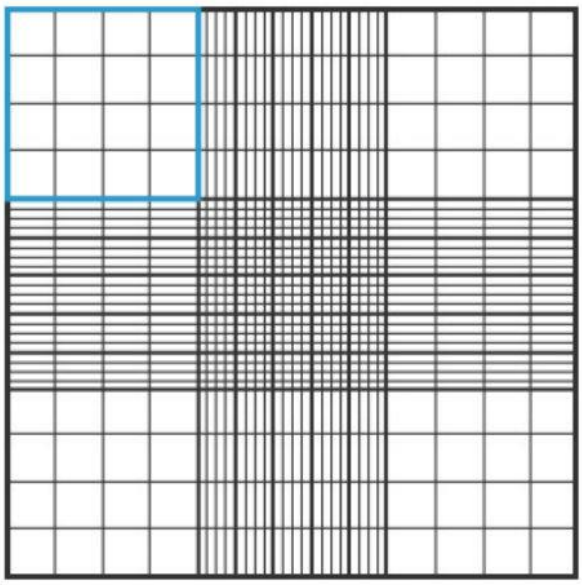

Formula 1:

*Density of the cells=the total cell number of 4 corners/4 *2*10^4*

The final diluted cells were seeded into the T75 flask (Biowest, France), and incubated at 37 °C in the CO_2 incubator. The medium was changed every 2 days. In order to purify the astrocytes and eliminate the microglia and oligodendrocyte, after 7 days when the cells were confluent, the T75 flask was shaken on a shaker at 240rpm for 6 hours, the supernatant containing the microglia was discarded, the astrocytes adhered on the bottom of the T75 flask was washed with HBSS twice and then did the first time second culture. Aspirated the HBSS and added 5ml 0.25% trypsin, 5 ml HBSS incubated at 37 °C in the CO2 incubator, checked the cells every 5 min until the astrocytes were detached from the bottom. Added 10ml medium (DMEM-F12+ 10%

heat-inactivated fetal bovine serum + 1% Penicillin/Streptomycin) to stop the digestion. Certificated the cells at 300 x g for 5min, aspirated the supernatant and added a new medium to resuspend the cells, detected the density of the cells, diluted into the 10^4 /mm with culture medium and seed the purified astrocytes into new T75 flasks. After in vitro cultured for another 4-5 days, did the second time second culture, the protocol was same as the first time the second culture and seeded the cells into T25 dishes. After in vitro cultured for 14 days, the astrocytes could be regarded as mature astrocytes, and are ready for the experiment.

Aβ application and Anesthetics exposure

The $A\beta_{1-42}$ (50ng) was kept in 1.5ml vial at -80°C. Dissolute the frozen $A\beta_{1-42}$ (50ng) by 110ul DMSO (Dimethyl sulfoxide, Sigma, USA) to make the concentration of $A\beta_{1-42}$ 100mm/ml, vortexed the vial for 1min. Put the vial into the ultrasonic cleaner (Bandelin, Germany) for 15min to make the $A\beta_{1-42}$ dissolved thoroughly. Prepared slices and in vitro cultured astrocytes were incubated in carbogen saturated aCSF for 90min before added the $A\beta_{1-42}$ and make the concentration of $A\beta_{1-42}$ to 50nm, then aerated the $A\beta_{1-42}$ existing aCSF with the following different mix gases respectively.

1. 65%Xenon (1.9mM in aCSF)+carbogen (95%O_2 +5%CO_2) for 60min
2. 1%isoflurane (370mm in aCSF) + carbogen (95%O_2 +5%CO_2) for 90min.

After exposure to those anesthetics, the slices and cells were gassed with carbogen for another 60/90min for the anesthetics washing out. The control groups were gassed only by carbogen.

Anesthetics exposure

The prepared slices and in vitro cultured astrocytes were incubated in carbogen saturated aCSF for 90min then aerated the aCSF with the following different mix gases respectively.

1. 65%Xenon (1.9mM in aCSF)+carbogen (95%O_2 +5%CO_2) for 60min
2. 1%isoflurane (370mM in aCSF) + carbogen (95%O_2 +5%CO_2) for 90min.

After the exposure to those anesthetics, the slices and cells were gassed with carbogen for another 60/90min for the anesthetics washing out. The control groups were gassed only with carbogen.

AAV mediated MEGF10 gen knock down

I used the AAV 9(Fig. 3) to deliver the small interfere RNA (siRNA) to the hippocampus to suppress the expression of MEGF10. The target sequence is: 805 - CCTGAGGGTCGCTTTGGAAAGAACTGTTC 2710 - GCAGACTATACCATCGCAGAAACCCTGCC 3136 -

TGCGGCTACGTGGAGATGAAGTCGCCGGC 3215 -
GGAATGTCTATGAAGTCGAACCTACAGTG

MEGF10 siRNA AAV9 ($4.72*10^{12}$ genome copies per mL) and control siRNA AAV9 ($3.56*10^{12}$ genome copies per mL) were produced by abm canada.

Stereotaxic injection was performed as before[95]. The injection micropipette: Hamilton syringe was placed into the holder of the stereotaxic arm, 2µl virus was withdrawn. At first, the 8-week-old adult male mouse was given 1 drop of Metamizol (Hexal® 500mg/ml, Germany) orally, and intraperitoneal injected 0.0025ml/g MMF (Midazolam Hexal®, 5mg/5ml, Germany; Medetomidine Sedator®, 1mg/ml Netherlands; and Fentanyl Fentadon®, 50ug/ml, Netherlands) (obtained from the ZPF of klinikum Rechtes der Isar). After it slept, the hair of the head was shaved, and intraperitoneal injected 0.0025ml/g Mannit (Serag Wiessner, 15%, Germany) . The mouse was placed in the apparatus, fixed the left ear bar, the scale was normally 42mm, gently positioned the mouse's head to lead its ear canal onto the ear bar, kept the mouse's head in place and slowly positioned the right ear bar and used the nose clamp to fix the nose in order to complete the fixation. The eyes of the mouse were protected by the ointment (Bepanthen, Bayer, Germany). Used one small tweezers onto the skull and move it to test whether the fixation successful or not. Used the skin disinfectant spray to sterilize the head, subcutaneous injected 2% lidocainhydrochlorid (Xylocain®2%), made an incision along the midline of the skull, cleaned the blood, separated the subcutaneous and muscle tissue under the dissection microscope. Marked

the bergma with a marker pen, and adjusted the X, Y-position of the bergma to 0 by bringing the tip of the Hamilton syringe to the position of the bergma. The coordinates of the dentate gyrus: 1.8 mm posterior to bregma, 1.2 mm lateral from midline and 1.65 mm dorsoventral from dura. Drilled the small holes with a bone scraper, the Hamilton syringe was infixed into the brain correctly by the coordinates, with the speed of 1mm/1min. Waited for 10min before injection. The speed of the injection was 50nl/min. Left the syringe in the site for an additional 10 min before withdrawn the syringe. Closed the muscle and the skin with Histoacryl (Braun, Germany). Subcutaneous injected 1 drop 2% lidocaine hydrochloride (Xylocain®2%) beside incisions and meditol was given orally for postoperative analgesia. 0.008ml/g AFN (Atipamezol Antisedan® 5mg/ml, Germany; Flumazenil Hexal® 0.1mg/ml, Germany; Naloxon Braunchy Melsung, 0.4mg/ml Germany) (obtained from the ZPF of klinikum Rechtes der Isar) was given intraperitoneally in order to wake up the mouse. And the mouse was kept under the red light for recovery warmly. And moved back to the mouse room after it recovered. The weight of the mouse was weighed every day after the surgery, and the meditol was given orally the first 3 days. After 3 weeks of recovery, the mice were sacrificed for the following experiments.

Fig 3 the map of the virus skeleton

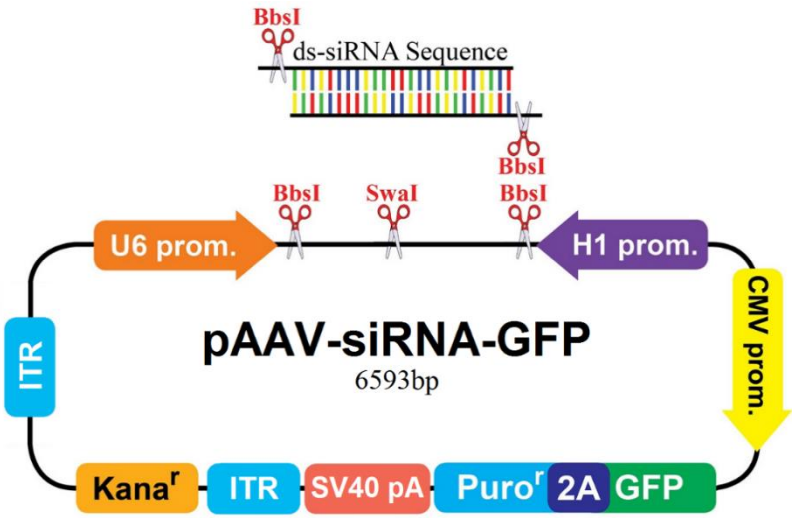

Fig 4 how to fix the mouse by using the ear bar[95]. (Fig4 is from the publication of Cetin A, et al 2006)

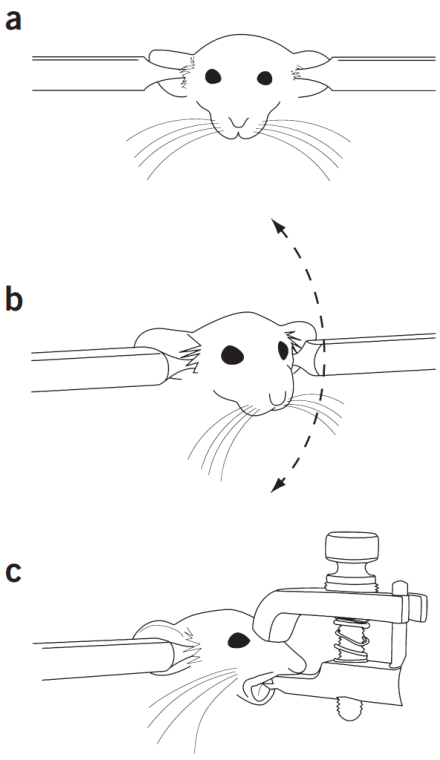

Protein preparation

After experiments, the in vitro cultured astrocytes were harvested by using the 1*laemmli, which was diluted from 5*laemmli (Table 5) with dH2O. The proteins were kept in vials and boiled at 95°C for 5min. After cooled down at the room temperature, the proteins were stored at -20°C before being used. The concentration of the protein samples was calculated and adjusted to be consistent at the first time western blot by using housekeeping protein and Image Lab software.

The protein of the brain slices was extracted by using the prepared lysis buffer (Table 6). All the following process were performed on ice or at 4°C. At first, the grinding tube (Biorad, USA) was centrifuged for 3min at 12000rpm, extracted the water out. 4-5 hippocampi were put inside one grinding tube, added 200µl lysis buffer, used the mini grinder to homogenize the tissues for 1min, the homogenized tissue was centrifuged for 30min at 12000rpm. The suspension was transferred to a new vial, and boiled at 95°C for 5min. After cooled down at the room temperature, the proteins were stored at -20°C before being used. The concentration of the protein was determined using the Pierce™ BCA® Protein Assay Kits and Reagents (Thermofisher, USA). After determination, the concentration of different proteins was adjusted by 4* or 2* sample buffer (Table 7) to be consistent. Every sample consisted of 30µg protein.

Table 5

5*Laemmli (10ml)

Substance	ml
1M Tris PH6.8	2
10% SDS	2.5
1M DTT	2
10% PHENOL RED	0.2
Glycerol	2
dH2O	1.3

Table 6

Substance	µl
RIPA(Sigma)	970
100 PMSF(Roche)	20
50complete	10
Peptains	1

200µl protein extraction buffer for 4-5 slices of hippocampus

Table 7

4*Sample buffer

Substance	µl
LDS 4*(Invitrogen™ Novex™ NuPAGE™, Thermofisher,USA)	1000

Reducing agentμμ(Invitrogen™ Novex™ NuPAGE™, Thermofisher,USA)	400

2*sample buffer

Substance	μl
4*sample buffer	500
dH2O	1300

Western blot

For western blotting, a total of 20μl of the sample was loaded per lane and 5μl the Novex™ Sharp Pre-stained Protein Standard (Thermofisher, USA) was loaded in the last lane. The proteins were electrophoretically separated on a 10% SDS-PAGE gel (Table 8) in the Elpho Buffer (Table 9). I used the constant voltage 100V for 20min and changed the voltage to 200V for another 45min in order that the band of MEGF10 (130KD) was totally separated. After the electrophoretic phase, I used the Image Lab stain-free gel to image the gels, and check whether the electrophoresis successful or not. Before transfer, the polyvinylidene fluoride membrane (Amersham Hybond LFP 0.2 PVDF Western blotting membrane, GE, USA) was soaked totally into methanol for 30 seconds and washed in dH2O for 30 seconds. The protein bands were transferred to the PVF membrane in the 1* transfer buffer (Table. 10) at constant 80V for 1 hour. After

transfer, the membrane was imaged by using the software Image Lab to get the image of the bands of total protein. After blocking with 1* Rotiblock (Biorad, USA) for 1 hour, the membrane was cut into two pieces according to the protein standard, in order that MEGF10 band (130KD) and GAPDH (38KD) band were separated. The membranes were incubated with Anti-MEGF10 antibody (Millipore USA, 1 : 500)+1*TBS/T (Table 10) and anti-GAPDH (CST,USA, 1:10000)+1*TBS/T 4°C overnight. On the next day, the membrane was first washed by 1*TBS/T 3 times, every time 10min. Subsequently incubated the membrane with horseradish peroxidase-conjugated secondary antibodies (CST, USA, 1:10000,) for 2 hours at room temperature. The membrane was washed by 1*TBS/T 3 times, every time 10min. The Clarity™ Western ECL Blotting Substrates (Biorad, USA) A and B were mixed equally, and the membrane was soaked into the mixed ECL for 1 min. Imaged the membrane by Imaging lab software. The bands were quantified by Imaging lab software[96].

Table 8

10%SDS-PAGE gel

separation gel:

Substance	
H_2O	4.1ml
Acrylamide/bis (30% 37.5:1; Bio-Rad)	3.3ml
Tris–HCl (1.5 M, pH 8.8)	2.5ml

SDS, 10%	100µl
N,*N*,*N*′,*N*′-tetramethylethylene-diamine (TEMED) (Thermofisher, USA)	10µl
Ammonium persulfate (APS), 10%	32µl

stacking gel:

Substance	
H_2O	6.1ml
Acrylamide/bis (30% 37.5:1; Bio-Rad)	1.3ml
Tris–HCl (1.5 M, pH 8.8)	2.5ml
SDS, 10%	100µl
N,*N*,*N*′,*N*′-tetramethylethylene-diamine (TEMED) (Thermofisher, USA)	10µl
Ammonium persulfate (APS), 10%	100µl

TEMED and APS were added to the solution when ready to pour.

Step:

1 pour the separation gel

1 pour the stacking gel

2 insert the comb to make wells carefully, avoiding the bubbles under the comb

3 leave for 30min

Table 9

Elpho buffer (2L)

Substance	
d H2O	2L
Tris	6g
Glycin	28.8g
SDS	2g

Table 10

Transfer buffer

Substance	
d H2O	1L
Tris	3g
Glycin	6.9g

Table 11

1*TBS/T (2L)

Substance	
d H2O	2L
Tris	6g
NaCl	22.2g

Tween 20	2ml

Quantification of dendritic spine density

After experiments, the 100mm GFP-M brain slices were transferred into the 6 well plate which had 1* PBS. Unfolded the slices and put nets and metal holders onside the slices, aspirated the PBS with a small plastic pipette and put 4%PFA (paraformaldehyde) inside the wells, kept it overnight at room temperature. The next day, washed the brain slices with 1* PBS 3 times, every time 10min. Used the little brush and tweezer to get the nets and holders out carefully. Took one 12 well plate, put 1* PBS inside every well. Transferred the slices into the 12 well plate with little brush. Aspirated the PBS with a plastic pipette. Incubated the brain slices with 1* PBS+0.5%Triton-X (Sigma-Aldrich, USA) +10%normal goat serum(Sigma-Aldrich, USA) (optimal 500ul/well) for 2 hours at room temperature on the shaker. After that the brain slices were incubated with 1* PBS+1:200GFP antibody (rabbit IgG Alexa Flur@488, Thermofisher, USA) (500µl/well) for 2 hours at room temperature in dark place. Washed the brain slices with 1* PBS 3 times, every time 10min after the incubation.

At last, every 3 slices were put onside one object slide and were mounted with Dako Fluorescence Mounting Medium (Dako north America, USA) and were covered

by coverslip carefully, avoiding the small air bubbles formed on the slices. Dried the slices in one dark box at the room temperature overnight, and used the nail polish to seal the sides of the coverslip. The slices could be stored at 4°C for 2-3 months.

The Zeiss confocal microscope was used to image the dendron of the neuron in dentate gyrus.

Step:

1 use the 10* objective to find one interesting region which contains several complete dendron,

2 change to 40* oil objective, choose one complete dendron, make it always in the middle of the screen, horizontal,

3 the range of the Z-stack is determined by the first and last version of the dendron, scan 12 slices of one dendron.

4 take pictures of 3 dendron, move to the other position, take another 3 pictures,

5 15 dendron are taken from one hippocampus.

After took all the pictures of the dendron, the black ZEN software was used to measure the dendritic spines density.

Steps:

1 load the confocal profile of the dendron,

2 use the tool ‘open Bezier’ to measure the length of the dendron,

3 use the tool ‘circle’ to circle the spines in different Z-stack slice,

4 calculate the dendritic spines density,

5 the average value of the spine density in one hippocampus is one “n” for statistical analysis.

Immunofluorescence

After being incubated with $A\beta_{1-42}$ and exposure to the anesthetics, the 100mm C57BL/6 brain slices were fixed by 4% PFA (paraformaldehyde) at room temperature over night as described before. The slices were then washed with 1* PBS, permeabilized and blocked with 0.3% Triton-X (Sigma-Aldrich, USA) and 10% normal goat serum (Sigma-Aldrich, USA) for 2 hours, then incubated with the first antibody, anti-GFAP (Abcam, USA, 1: 1000, chicken), anti-synaptophysin (Abcam, USA, 1: 200, rabbit), anti-PSD95 (CST, USA, 1: 200, rabbit), at 4°C overnight. The following day, the slices were labeled with the second antibody, (donkey anti-chicken Alexa fluor594, Thermofisher, USA, 1: 500, donkey anti-rabbit Alexa fluor488, Thermofisher, USA, 1: 500) at room temperature for 2 hours keeping in dark. The slices were mounted with Dako mounting medium (Dako north America, USA).

The Zeiss Apotome microscope was used to image X, Y, Z-stack of the dentate gyrus of the hippocampi. The objective was 60*oil. 3 positions of each DG region were taken. The range of the Z-stack was determined by the first and last version of the cells. Scan 10slices of one cell. The colocalization of the synaptophysin or PSD95 and GFAP was quantified by using the plugin ‘colocalization finder’ of the software Fiji. The

Pearson's correlation coefficient value was used to present the colocalization[97]. The average "Pearson's R" value of one hippocampus was used as one statistical "n".

Statistical analysis

If the data distributed normally, an unpaired t-test was performed. Data were expressed as the mean ± SD. If the data didn't distribute normally, a Mann-Whitney U test was performed, and data were presented as median(IQR). $P<0.05$ was considered to indicate a statistically significant difference.

III Results

3.1 part i: the effect of isoflurane and xenon on the synapse loss through MEGF10 pathway

Isoflurane reduced dendritic spine density in the dentate gyrus

After exposing the GFP-M brain slices to 1% isoflurane for 90min, the dendritic spines density of the neurons in the dentate gyrus was quantified. The result showed that compared to control, 1% isoflurane could reduce the dendritic spine density. To resemble the clinical situation and observe whether this reduction is persistent or not, I also tested the spines density after another 90min's isoflurane washout. The results showed the reduction did not reverse. (Fig 5)

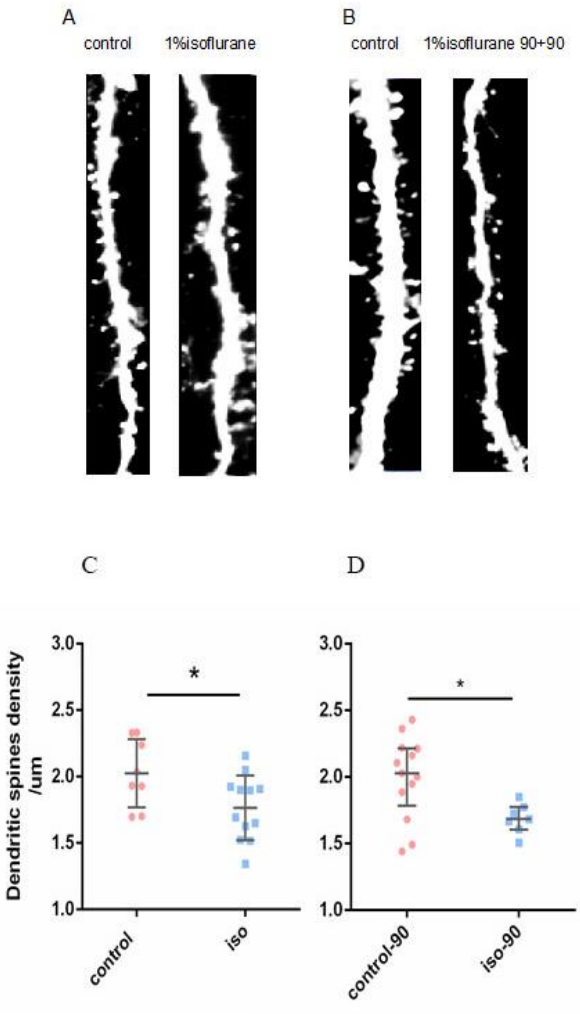

Fig 5: *Isoflurane reduced the dendritic spine density in the dentate gyrus of hippocampus. (A, C) spine density decreased significantly, after the brain slices were exposed to 1%isoflurane for 90min. (t-test, *P<0.05). (B, D) 90min after removal of isoflurane, the dendritic spines density did not recover. (Mann-Whitney U test, *P<0.05)*

Xenon could reduce the dendritic spines density reversibly

We gassed the GFP-M brain slices with 65%xenon for 60min and detected that the spines density decreased at the end of the exposure, and slightly reversed after another 60min xenon washing out. (Fig 6)

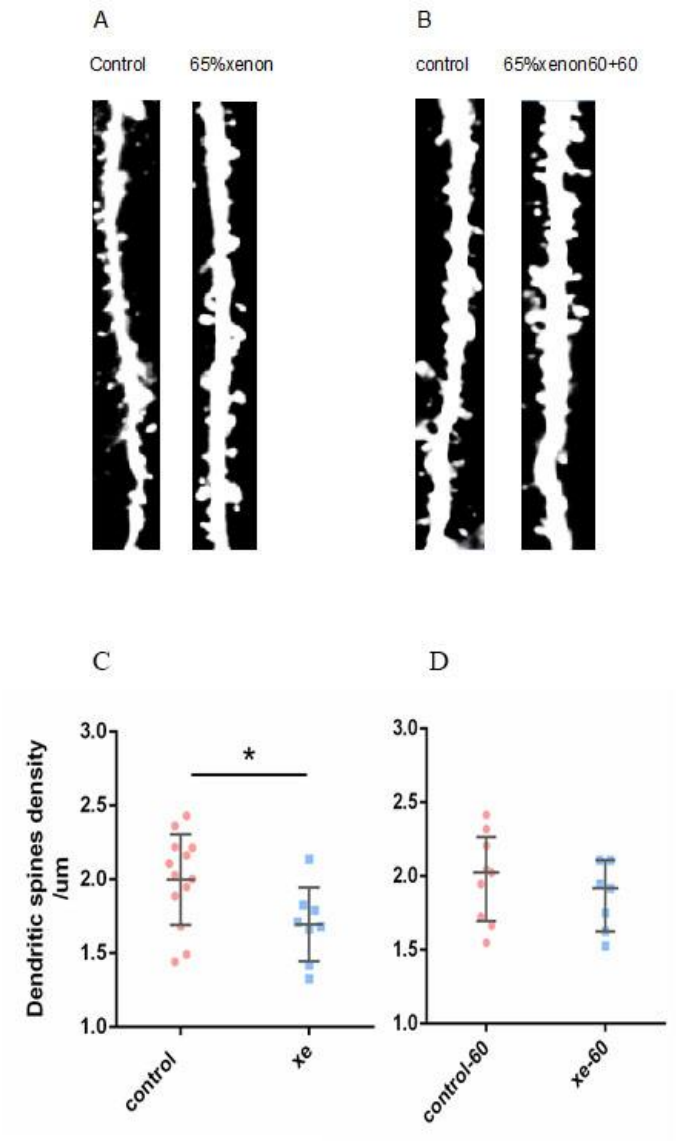

Fig 6*: Xenon (65%) reduced spine density reversibly. (A, C) the dendritic spines density of the neurons in hippocampus decreased after the exposure to 65% xenon for 60min. (t-test, *P<0.05) 6BD but when the xenon was washed out of the aCSF for another 60min, the effect of xenon on the dendritic spine reduction had been reversed. (Mann-whitney U test, P>0.05)*

Both isoflurane and xenon could reduce the expression of MEGF10 in cultured astrocytes

Next, I tested the MEGF10 protein expression in the in vitro cultured astrocytes.

After exposure to 1%isoflurane for 90min, the expression of MEGF10 has not changed. But 90min after the removal, the expression of MEGF10 was down-regulated compared to the control group. (Fig 7A. B)

The same phenomenon was also observed when the cells were gassed by 65%xenon. The significant decrease was observed 60min after 65%xenon exposure. (Fig 7C. D)

A

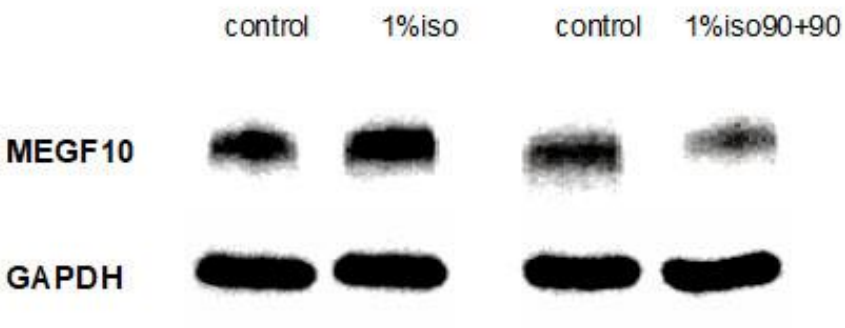
control
1%iso
control
1%iso90+90
MEGF10
GAPDH

B

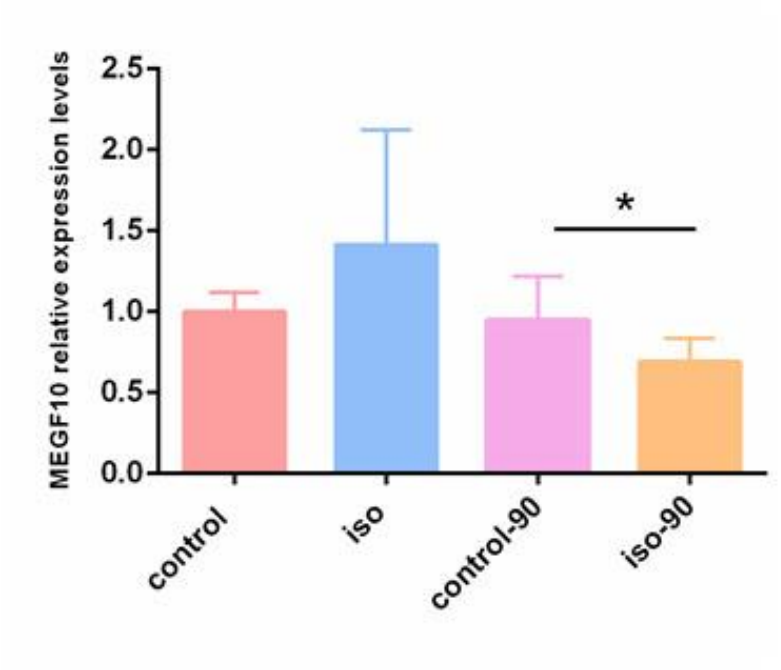
MEGF10 relative expression levels
2.5
2.0
1.5
1.0
0.5
0.0
*
control
iso
control-90
iso-90

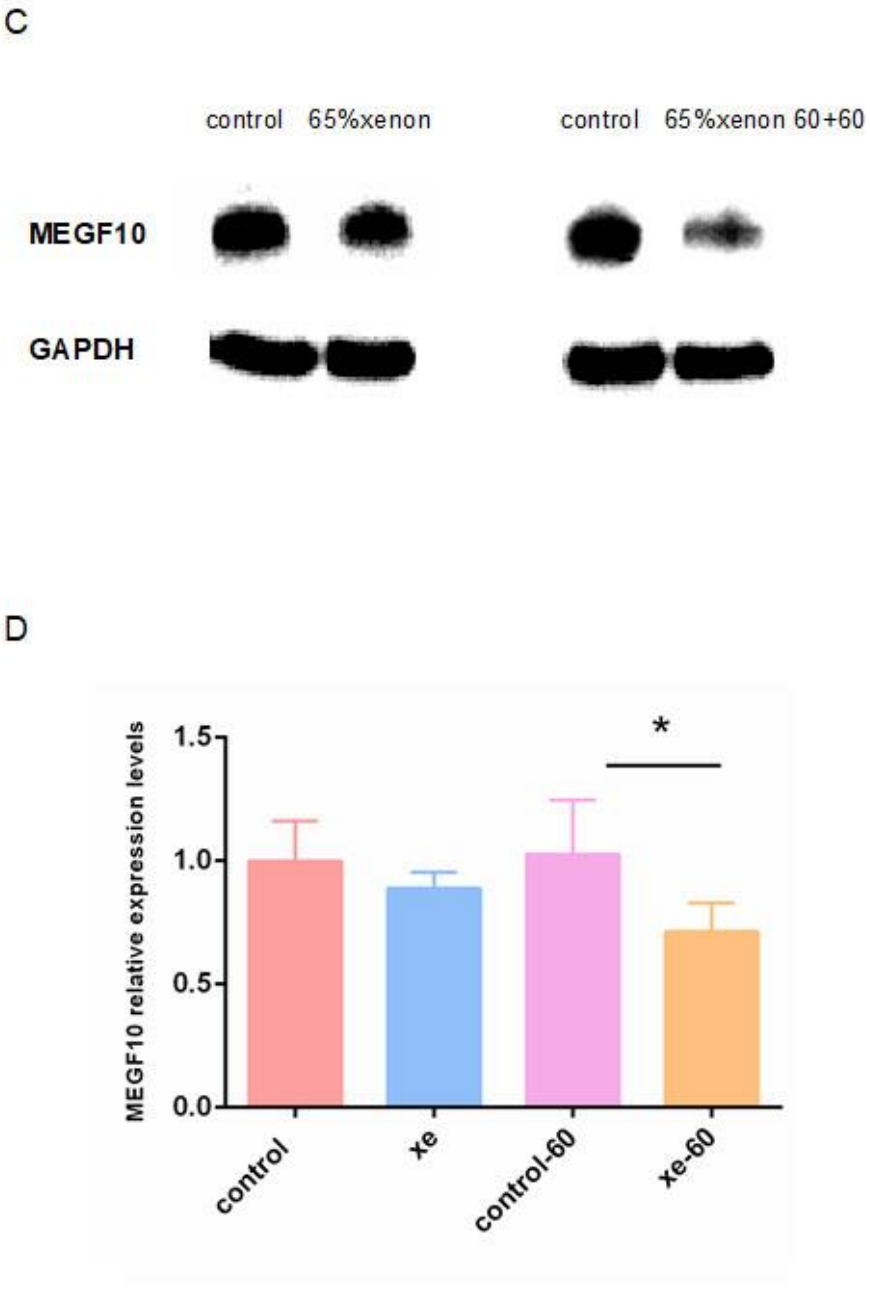

Fig 7: *Both isoflurane and xenon could reduce the expression of MEGF10 on the in-vitro cultured astrocytes. AC the membranes of MEGF10 and GAPDH. AB after gassed the cells with 1%isofllurane for 90min, the expression of MEGF10 didn't change (t-test, P>0.05), the decrease happened 90min after the isoflurane washing out (t-test, *P<0.05). CD after the exposure to 65%xenon, the expression of MEGF10 didn't change (t-test, P>0.05), 60min after the xenon washing out, the expression decreased (t-test, *P<0.05).*

The synapses were engulfed by the astrocytes in the dentate gyrus

The following pre-and post-synaptic markers were used in this study: synaptophysin and PSD95 to label the pre-and post-synaptic elements, and the GFAP to mark the astrocytes. The images were taken using an apotome microscope. Subsequently, the pre– and postsynaptic marker which were inside the astrocytes were estimated by analysing the co-localization coefficient of synaptophysin, PSD95, and GFAP. The imaging showed that the pre-(Fig.8A) and post-(Fig. 8B) synaptic components were inside the astrocytes, revealing that the astrocytes engulfed the synapses in the hippocampus.

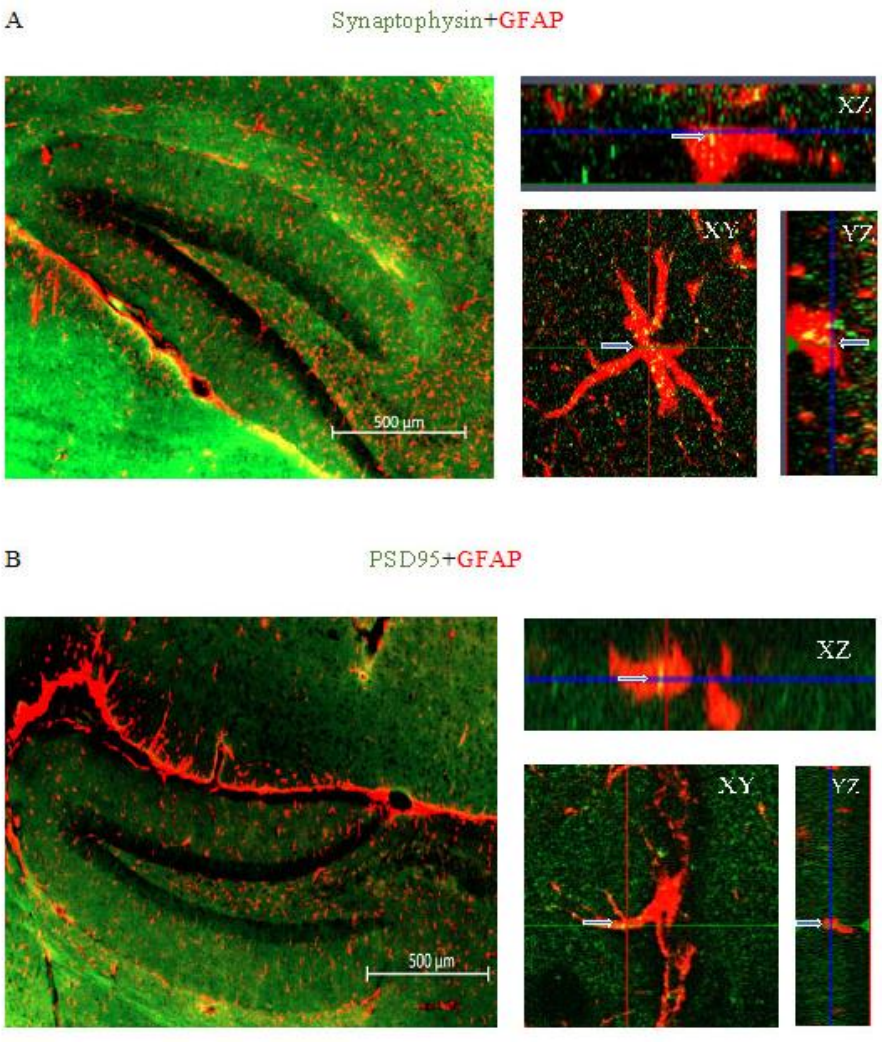

Fig 8: *The synapses were engulfed by the astrocytes in the hippocampi slices. 8A apotome images showing that the presynaptic marker(green) synaptophysin are inside the astrocyte (red). The arrowhead points the synaptophysin inside the astrocyte in the XY, YZ, XY phases (yellow). Fig 8B indicates apotome images showing that the postsynaptic marker (green) PSD95 are inside the astrocyte(red). The arrowhead points the PSD95 inside the astrocyte in the XY, YZ, XY phases (yellow). Those pictures reveal that both pre- and postsynaptic elements are inside the astrocyte, which may imply that the synapses are "eaten" by astrocyte.*

Isoflurane did not affect physiological synapse engulfment

After being gassed with 1%isoflurane for 90min, I tested the amount of the synapses inside the astrocytes by immunofluorescence. The synapses were labeled by pre-and postsynaptic marker: synaptophysin and PSD95. The colocalization of GFAP and the synapse markers in the astrocytes was used to quantify the engulfed synapses by astrocytes. And the results revealed that compared with the control, isoflurane did not change the engulfment of synapses by astrocytes (Fig 9A). After another 90min isoflurane washing out, there was also no change of this engulfment. (Fig 9B)

A

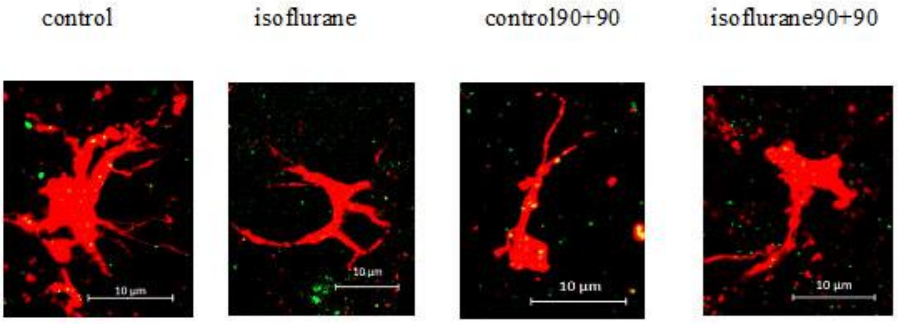
control
isoflurane
control90+90
isoflurane90+90
10 μm
10 μm
10 μm
10 μm

a b c d

B

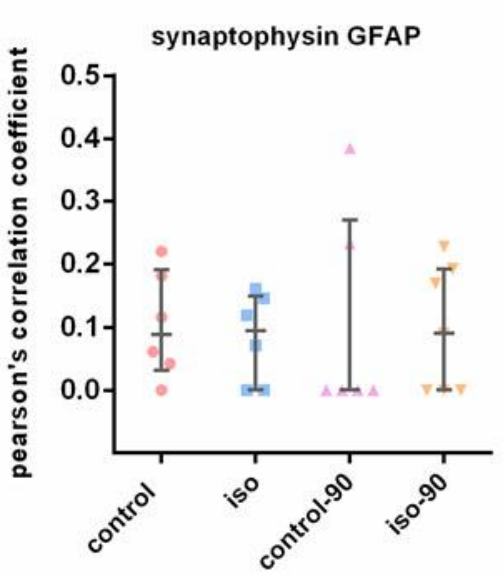
synaptophysin GFAP
pearson's correlation coefficient
0.5
0.4
0.3
0.2
0.1
0.0
control
iso
control-90
iso-90

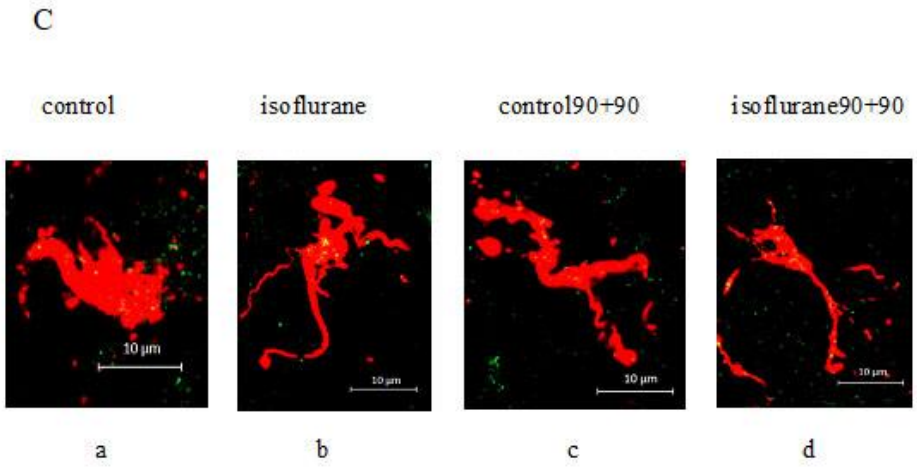

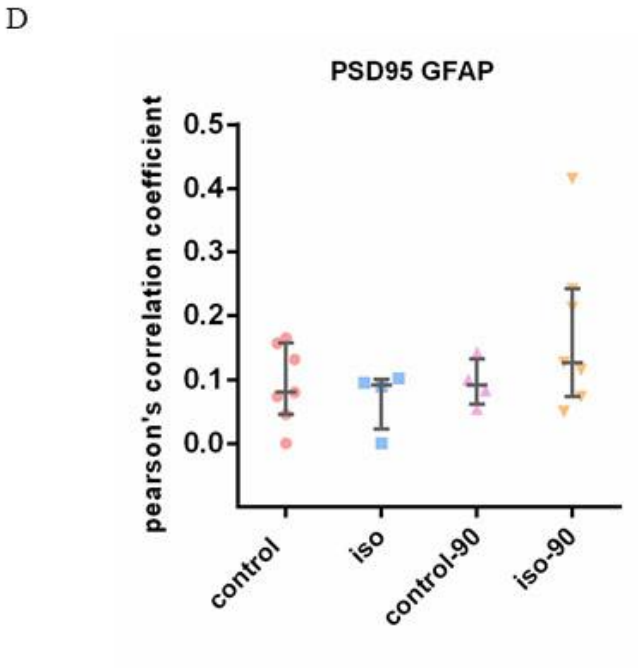

Fig9: *Isoflurane could not change the engulfment of synapses by astrocytes. the images of GFAP and synaptophysin(9A)/PSD95(9C): the red signal is GFAP; the green signal is synaptophysin(9A)/PSD95(9C); the yellow points inside the GFAP are the pre-(6A)/postsynaptic(9C) elements engulfed by astrocytes. 9B/9D it reveals that compared with the control there is no significant change of the synapses inside the astrocytes after treated with 1%isoflurane. Mann-whitney u test, P>0.05.*

Xenon (65%) did not change the elimination of synapses by astrocytes

The effect of 65%xenon on the elimination of synapses by astrocytes was tested after the brain slices were exposed by 65%xenon for 60min, and also after 60mins' xenon washing out. The results of the colocalization of GFAP and synaptophysin, PSD95 showed that being gassed by 65%xenon for 60min, the number of synapses inside the astrocytes had no change compared with the control group (Fig 10A), and the same results were also observed after another 60min xenon washing out (Fig 10B).

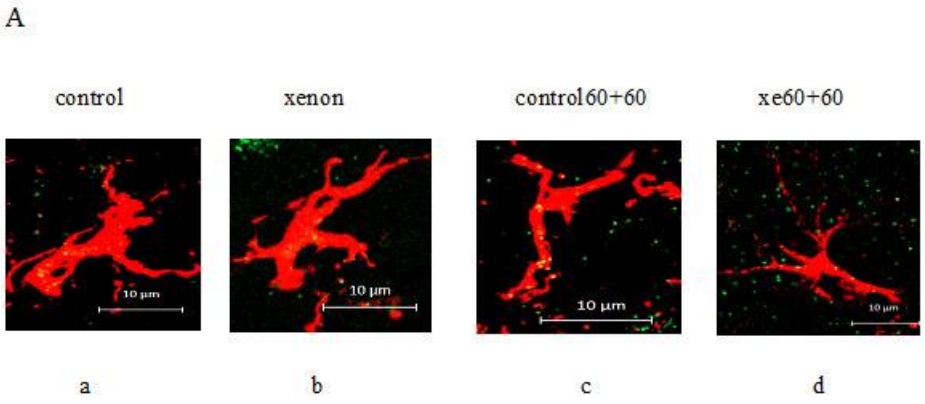

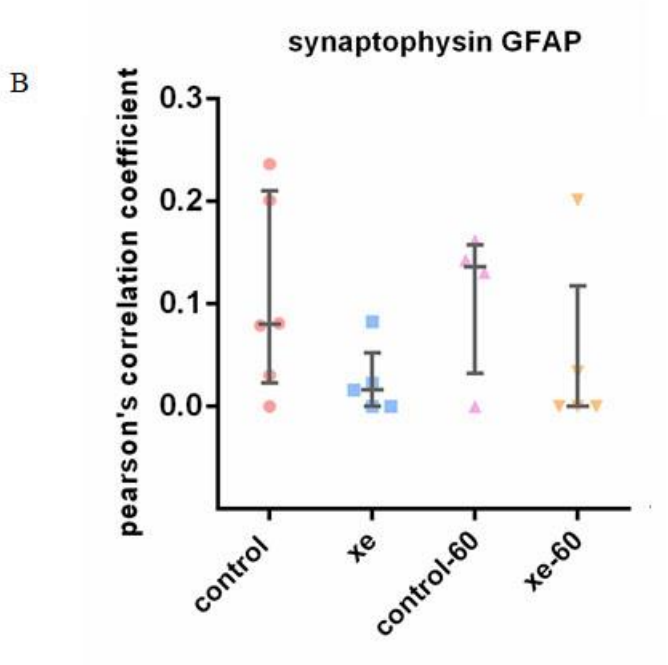

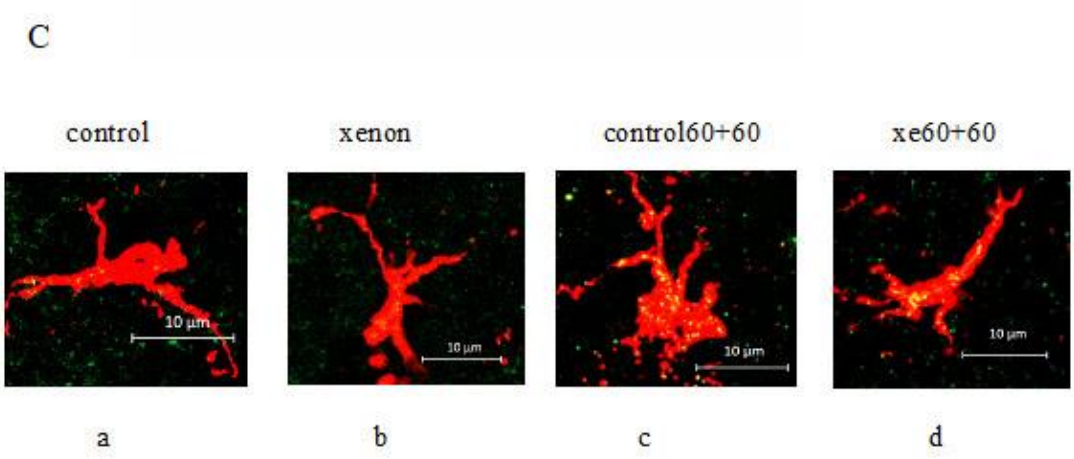

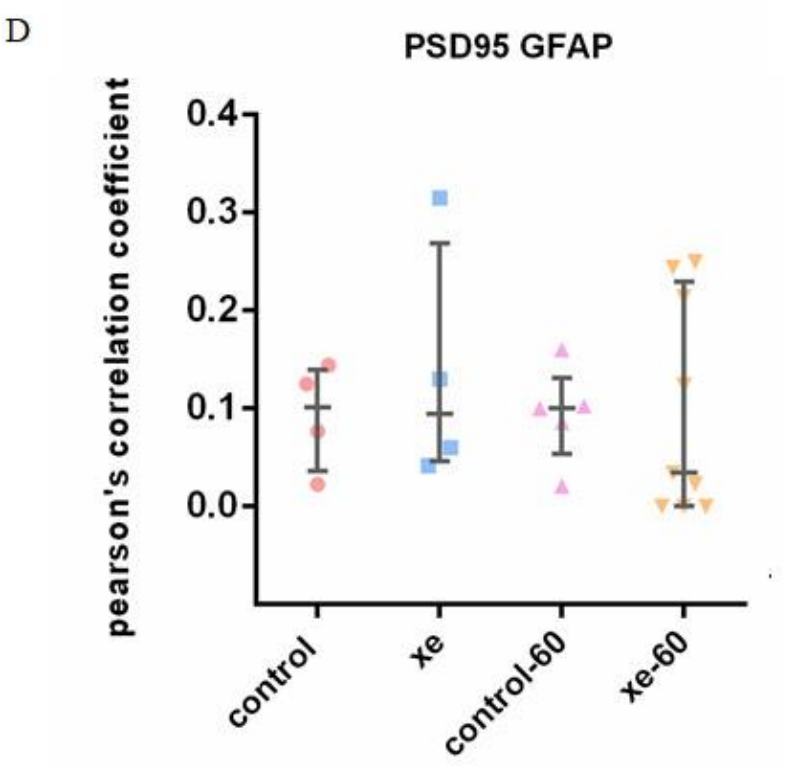

Fig10: *Xenon could not change the engulfment of synapses by astrocytes. the images of GFAP and synaptophysin(10A)/PSD95(10C): the red signal is GFAP; GFAP are the pre-(10A)/postsynaptic(10C) elements engulfed by astrocytes. 10B/10D it reveals that compared with the control there is no significant change of the synapses inside the astrocytes after treated with 1%isoflurane. Mann-whitney u test, P>0.05.*

3.2 part ii：isoflurane and xenon reverse the effect of $A\beta_{1-42}$ on the dendritic spine density through MEGF10 pathway

$A\beta_{1-42}$ decreased dendritic spines density

I measured the dendritic spines density after treating the GFP-M brain slices with 50nM $A\beta_{1-42}$. Compared with the control group, $A\beta_{1-42}$ decreased the dendritic spines density significantly (Fig.11B)

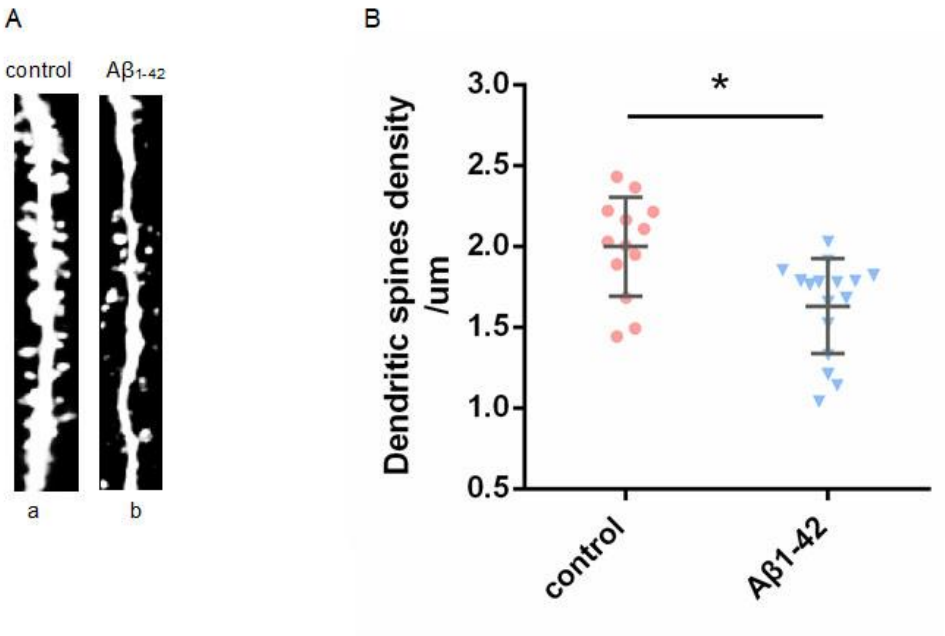

Fig. 11: *$A\beta_{1-42}$ decreased dendritic spines density. 11A(a) one dendrite from the control group, 11A(b) one dendrite from the $A\beta_{1-42}$ treated group. 11B, compared with the control group, the dendritic spines density of the $A\beta_{1-42}$ treated group had significant decrease. T-test, *P<0.05.*

The combined application with either isoflurane or xenon reversed the decrease of dendritic spines density caused by $A\beta_{1-42}$.

The $A\beta_{1-42}$ pre-treated brain slices were gassed with 1%isoflurane for 90min. After another 90min isoflurane washing out, I found that the dendritic spines density has been reversed (Fig.12B).

I also aerated 65%xenon to the $A\beta_{1-42}$ treated brain slices for 60min. And after another 60min xenon washing out, the dendritic spines density recovered (Fig.12D).

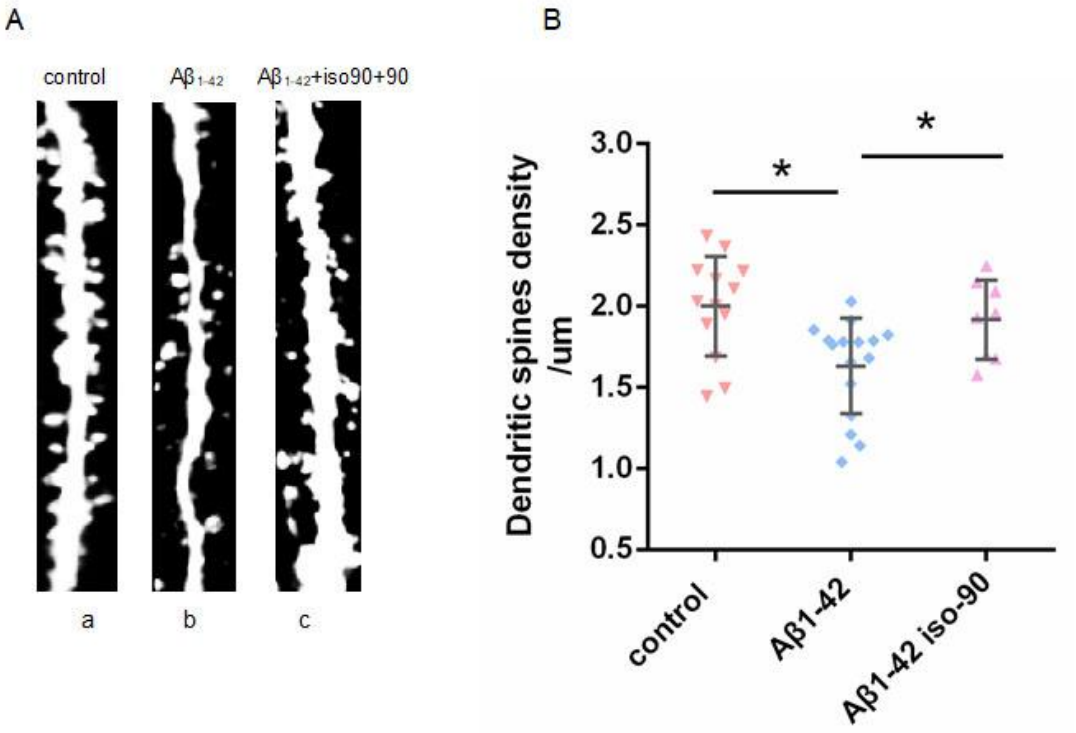

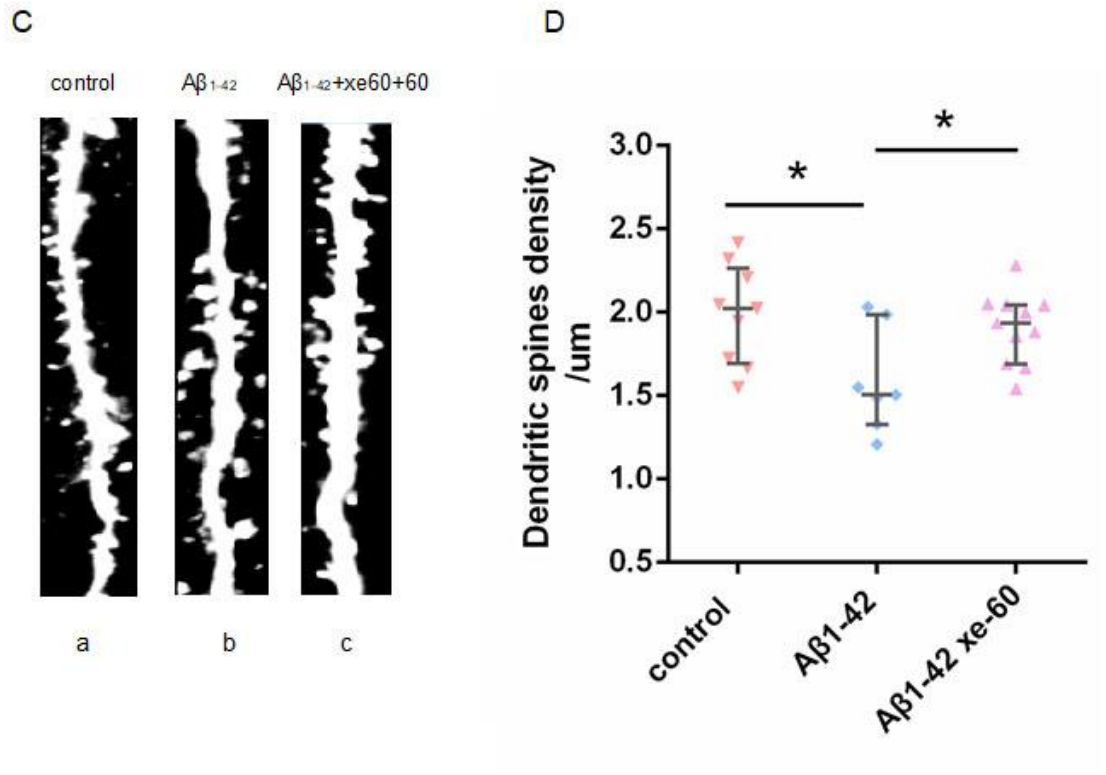

Fig 12: *The combined application with either isoflurane or xenon reversed the decrease of dendritic spines density caused by $A\beta_{1-42}$. 12A(a) one dendrite from the control group, 12A(b) one dendrite from the $A\beta_{1-42}$ treated group, 12A(c) one dendrite from the $A\beta_{1-42}$ combined with isoflurane group. 12B, compared with the only with $A\beta_{1-42}$ treated group, the dendritic spines density of the $A\beta_{1-42}$ combined with isoflurane group has a significant increase, t-test, *P<0.05. 12C(a) one dendrite from the control group, 12C(b) one dendrite from the $A\beta_{1-42}$ treated group, 12C(c) one dendrite from the $A\beta_{1-42}$ combined with xenon group. 12D, compared with the only with $A\beta_{1-42}$ treated group, the dendritic spines density of the $A\beta_{1-42}$ combined with xenon group has a significant increase, the effect of $A\beta_{1-42}$ on the dendritic spines has been reversed. Mann-whitney U test, *P<0.05.*

The synapses were engulfed by the astrocytes in the hippocampi slices

The pre-and post-synaptic markers were used in this study: synaptophysin and PSD95 to label the pre-and post-synaptic elements, and the GFAP to mark the astrocytes. The images were taken using an apotome microscope. Subsequently, the

pre– and postsynaptic marker which were inside the astrocytes were estimated by analysing the co-localization coefficient of synaptophysin, PSD95 and GFAP. The imaging showed that the pre-(Fig.8A) and post-(Fig. 8B) synaptic components were inside the astrocytes, revealing that the astrocytes engulfed the synapses in the hippocampus.

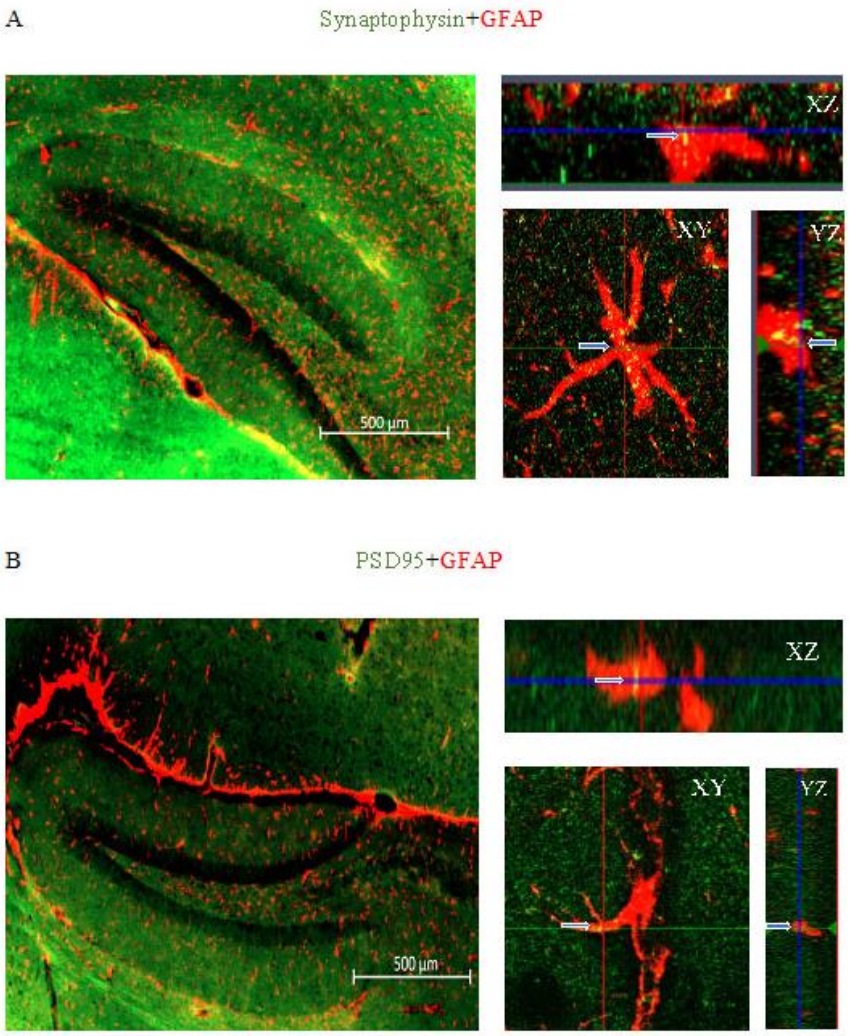

Fig13: *The synapses were engulfed by the astrocytes in the hippocampi slices. 13A it shows that the presynaptic marker (green) synaptophysin are inside the astrocyte (red). The arrowhead points the synaptophysin inside the astrocyte in the XY, YZ, XY phases (yellow). 13B it shows that the postsynaptic marker(green) PSD95 are inside the*

astrocyte (red). The arrowhead points the PSD95 inside the astrocyte in the XY, YZ, XY phases (yellow). Those pictures reveal that both pre- and postsynaptic elements are inside the astrocyte, which may imply that the synapses are "eaten" by astrocyte.

Aβ1-42 elevated pre- and postsynaptic marker inside astrocytes

After being incubated with 50nM Aβ1-42, there were more pre- and postsynaptic markers inside the astrocytes (Fig.14). Student's t-test revealed a significantly different compared with the control (pre 14B; post 14D).

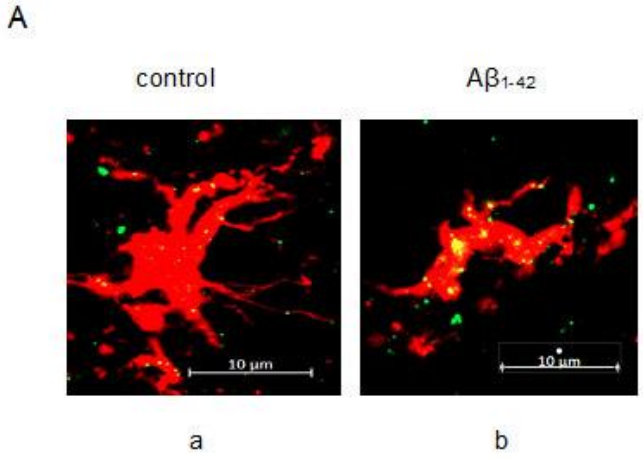

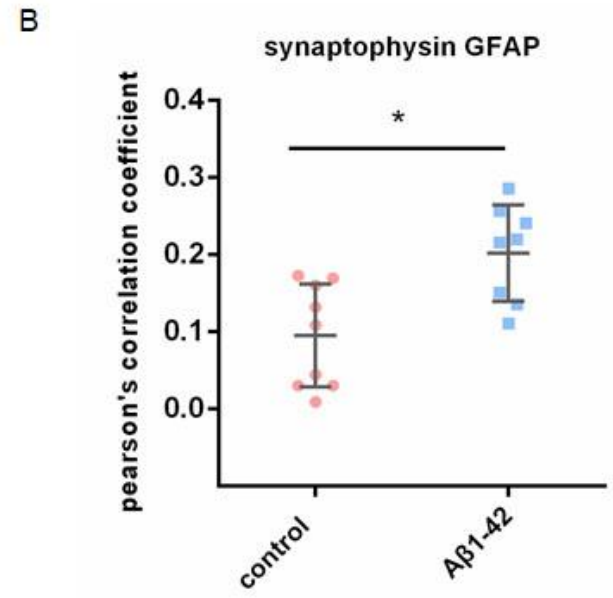

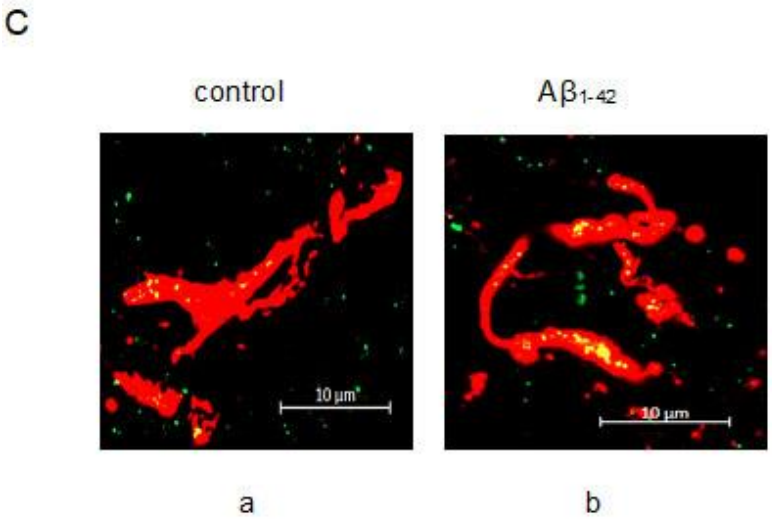

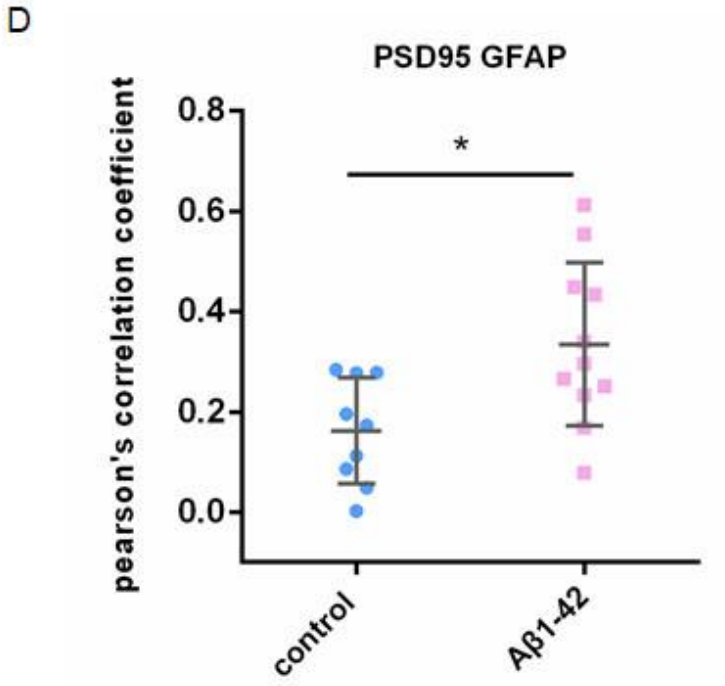

Fig 14: *$A\beta_{1\text{-}42}$ elevated pre- and postsynaptic marker inside astrocytes. 14A (a, b) the red signal is astrocyte (GFAP), the green is presynaptic marker (synaptophysin), the yellow points inside the astrocyte are synaptophysin. 14B it shows that there are more synaptophysin inside the astrocyte when treated with $A\beta_{1\text{-}42}$. T-test, *P<0.05. 14C (a, b) the red is also astrocyte, the green points are postsynaptic marker (PSD95), the yellow inside the astrocyte are the postsynaptic elements which are labelled by PSD95. 14D it reveals that $A\beta_{1\text{-}42}$ elevated postsynaptic marker inside astrocytes. T-test, *P<0.05.*

The combined application with either isoflurane or xenon reversed elevation of pre- and postsynaptic marker inside astrocytes

The $A\beta_{1-42}$ treated brain slices were exposed to 1%isoflurane for 90min. After another 90min isoflurane washing out, I analyzed the colocalization coefficient of synaptophysin (pre-), PSD95 (post-) and GFAP. Compared with the $A\beta_{1-42}$ group, there were less pre- and postsynaptic markers inside the astrocytes (Fig.15A, B, pre; 15C, D post).

I also aerated the 65%xenon to the $A\beta_{1-42}$ treated brain slices for 60min. After another 60min xenon washing out, I got the same results as isoflurane exposure experiment. Compared with the $A\beta_{1-42}$ the pre- and postsynaptic elements inside the astrocytes decreased significantly (Fig. 15E, F, pre; 15G, H, post).

A

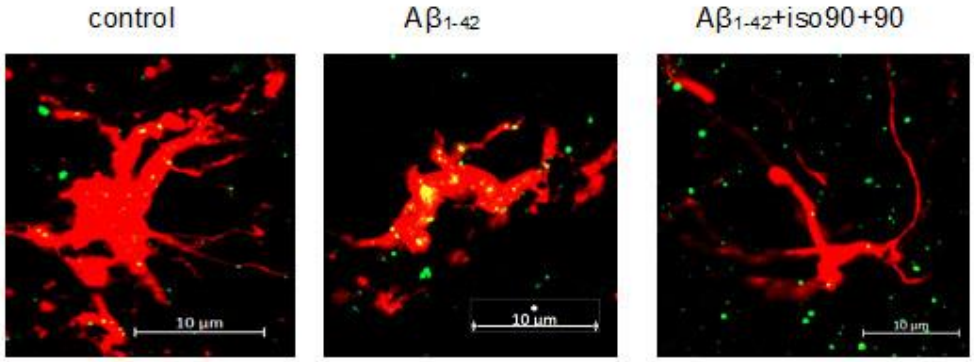
control
Aβ1-42
Aβ1-42+iso90+90
10 µm
10 µm
10 µm

a b c

B

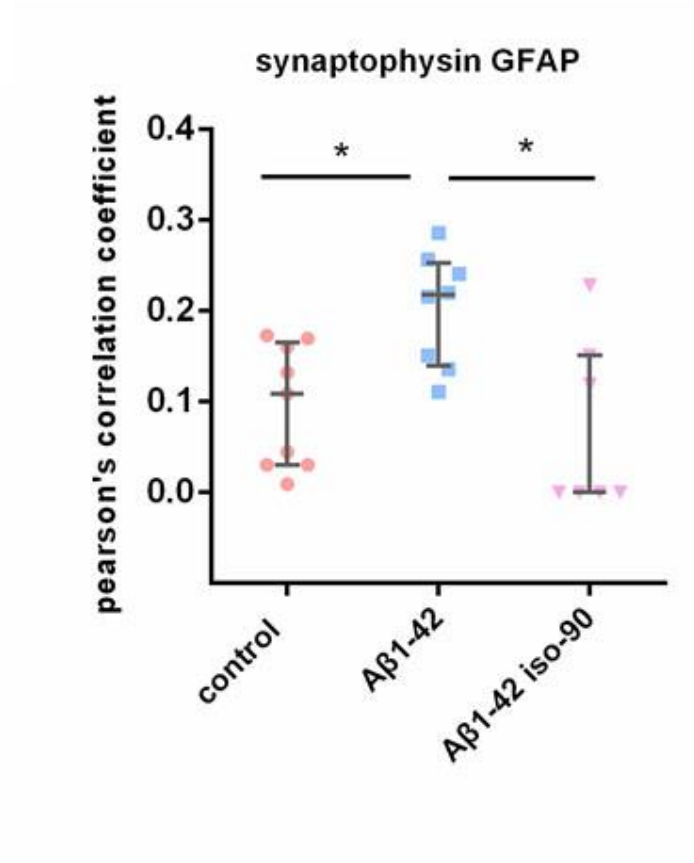
synaptophysin GFAP
pearson's correlation coefficient
0.4
0.3
0.2
0.1
0.0
*
*
control
Aβ1-42
Aβ1-42 iso-90

C

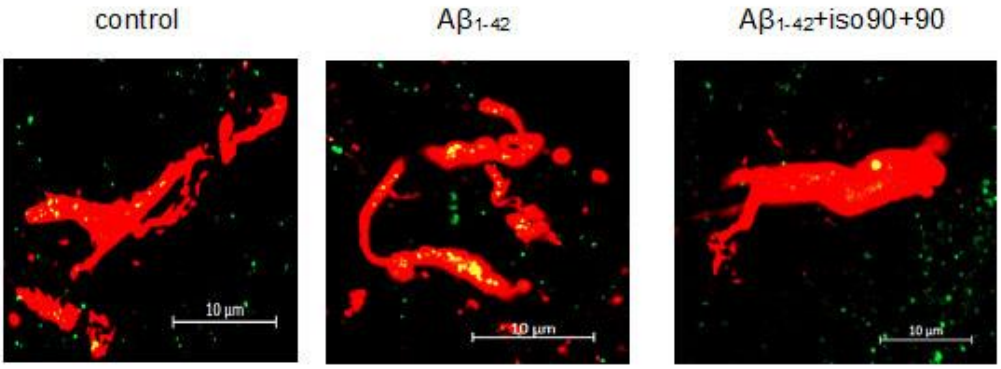
control
Aβ1-42
Aβ1-42+iso90+90
10 µm
10 µm
10 µm

a b c

D

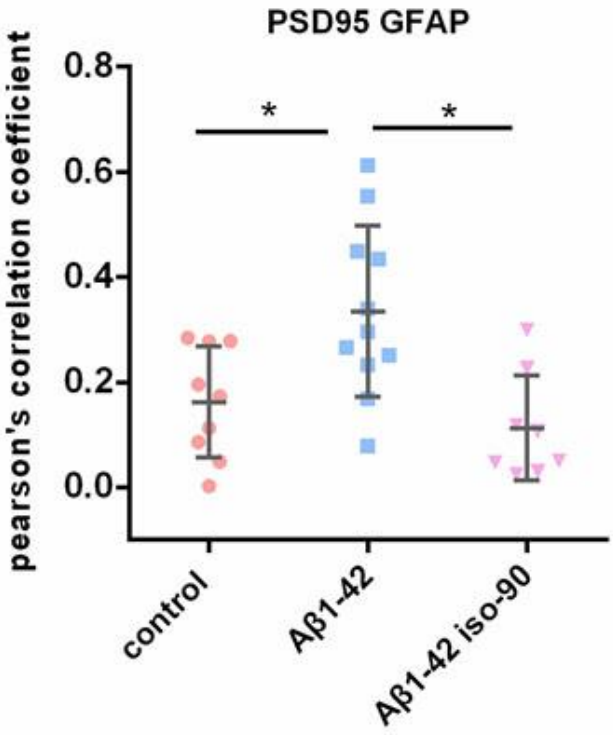
PSD95 GFAP
pearson's correlation coefficient
0.8
0.6
0.4
0.2
0.0
*
*
control
Aβ1-42
Aβ1-42 iso-90

E

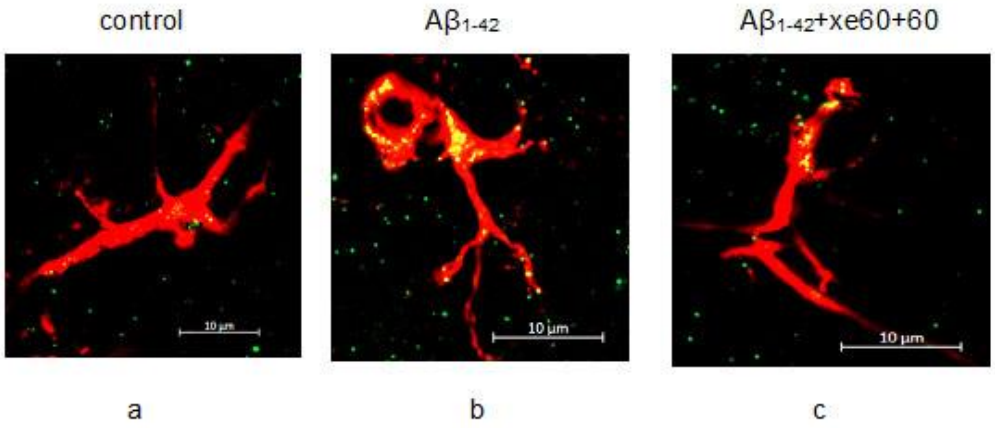
control
Aβ1-42
Aβ1-42+xe60+60
10 µm
10 µm
10 µm

a b c

F

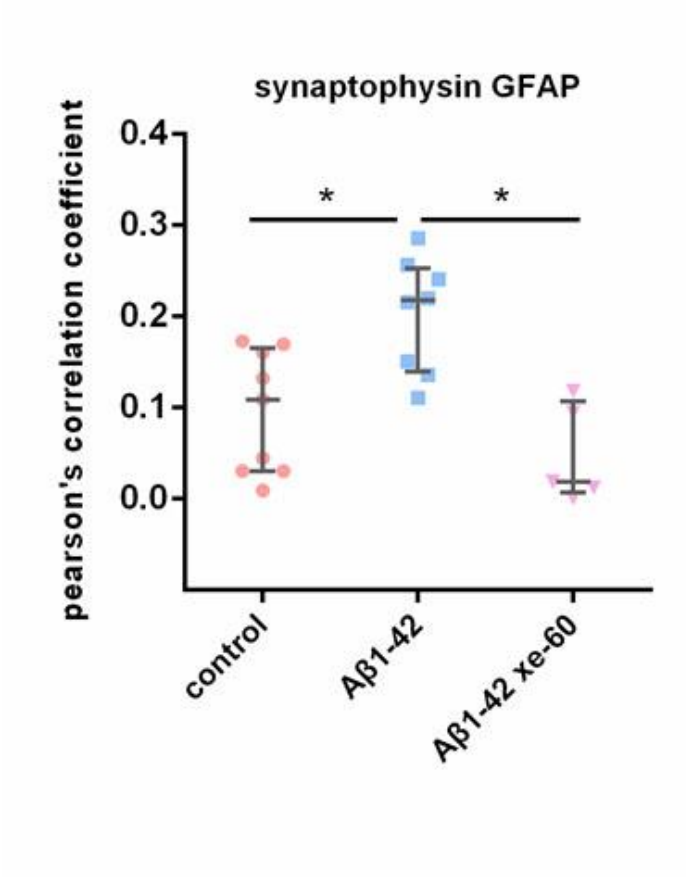
synaptophysin GFAP
pearson's correlation coefficient
0.4
0.3
0.2
0.1
0.0
*
*
control
Aβ1-42
Aβ1-42 xe-60

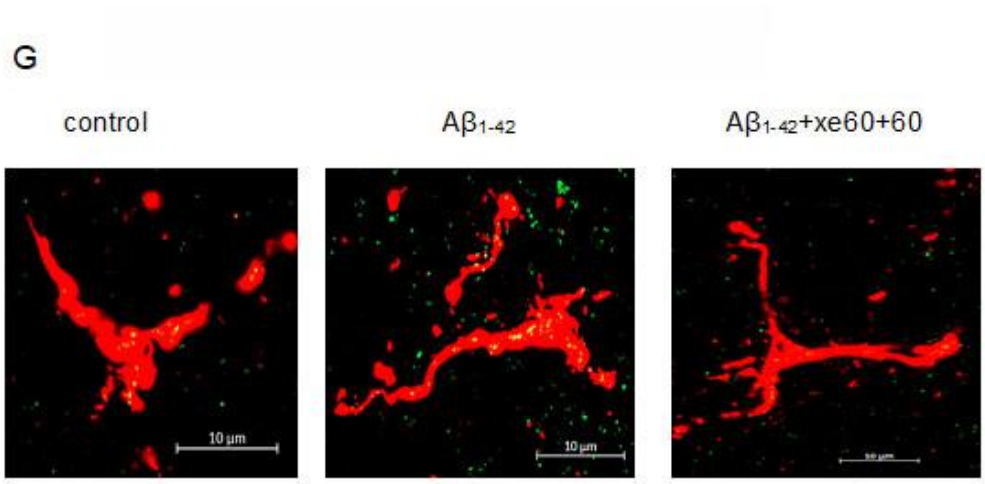

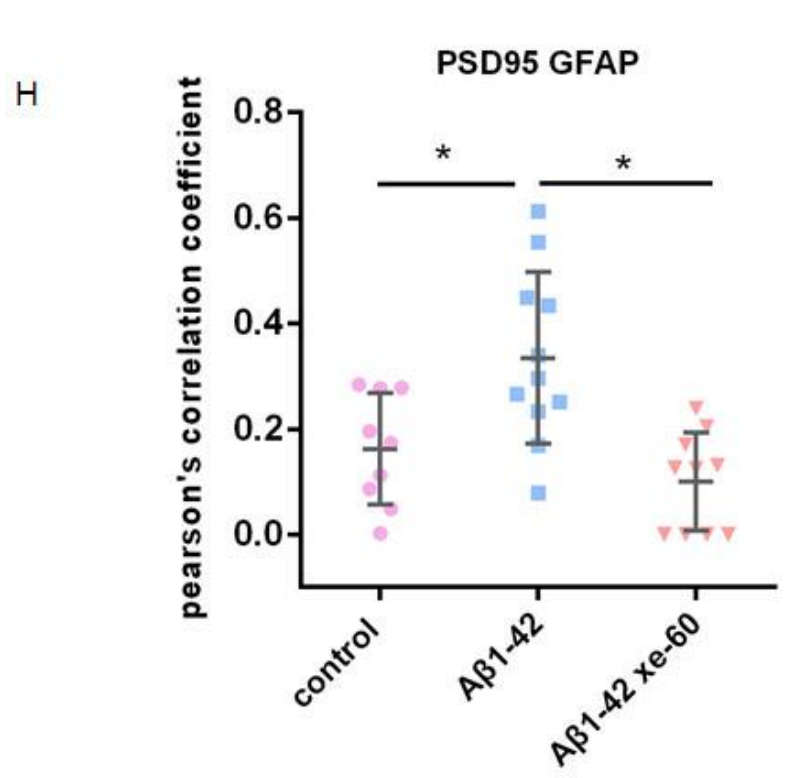

Fig 15: *The combined application with either isoflurane or xenon reversed elevation of pre- and postsynaptic marker inside astrocytes. 15A, E (a, b, c) the red signal is astrocyte (GFAP), the green is presynaptic marker(synaptophysin), the yellow points inside the astrocyte are presynaptic elements which are labelled by synaptophysin. 15B, F it reveals that after combined with isoflurane (B, Mann-whitney U test, *P<0.05), or*

*xenon (F, Mann-whitney U test, *P<0.05), there are significant reversal of the elevation of presynaptic elements inside the astrocytes. 15C, G (a, b, c) the red signal is astrocyte (GFAP), the green is postsynaptic marker (PSD95), the yellow points inside the astrocyte are postsynaptic elements which are labelled by PSD95. 15D, H it shows that both isoflurane (D, t-test, *P<0.05) and xenon (H, t-test, *P<0.05) could reverse the effect of $A\beta_{1-42}$ on the engulfment of postsynaptic elements by astrocyte.*

In the presence of $A\beta_{1-42}$ both isoflurane or xenon decreased MEGF10 expression in astrocytes.

I tested the MEGF10 protein expression in cultured astrocytes in the presence of $A\beta_{1-42}$.

After exposure to 1%isoflurane, the expression of MEGF10 was down-regulated compared to the $A\beta_{1-42}$ control group (Fig.16A).

The same phenomenon was also observed when the cells were gassed by 65%xenon. The decrease had a significant difference (Fig.16B).

A

a

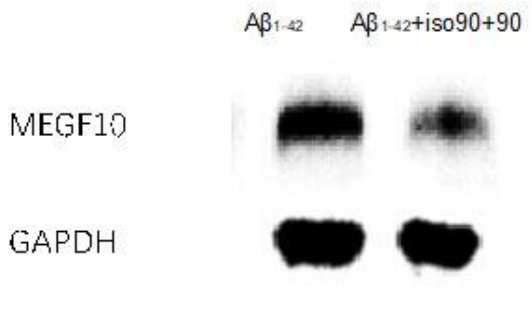
Aβ1-42
Aβ1-42+iso90+90
MEGF10
GAPDH

b

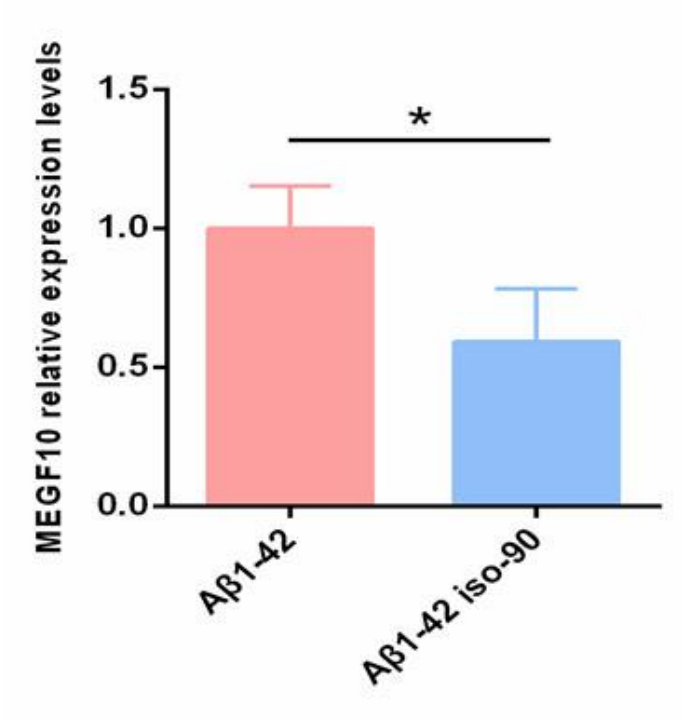
MEGF10 relative expression levels
1.5
1.0
0.5
0.0
*
Aβ1-42
Aβ1-42 iso-90

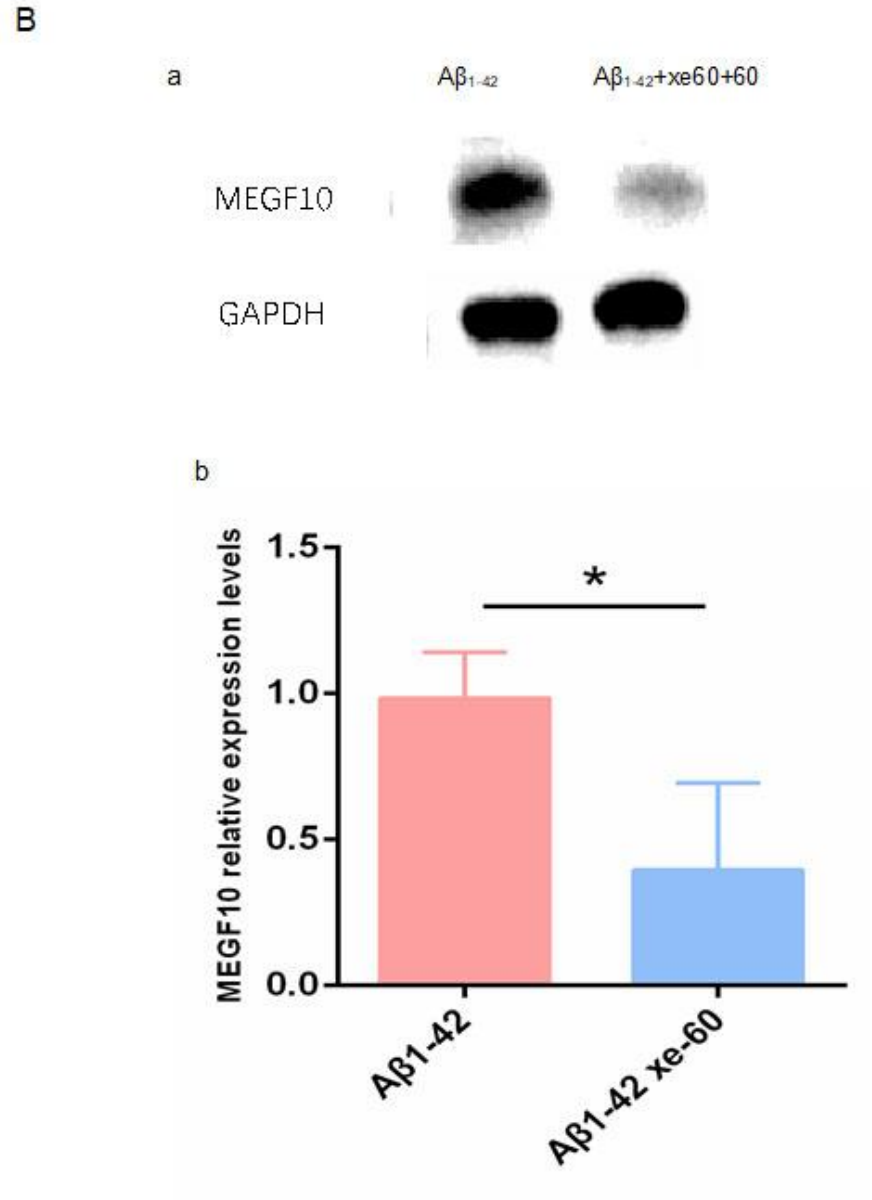

Fig 16: *Both isoflurane or xenon decreased MEGF10 expression in astrocytes in the presence of $A\beta_{1-42}$. 16A(a), B(a) the western blot membrane of the $A\beta_{1-42}$ treated cells and combined with isoflurane (Aa) or xenon (Ba). GAPDH serves as the loading control. 16A(b), B(b) quantitative analysis of the membrane shows that when treated with $A\beta_{1-42}$ combined with isoflurane (Aa, t-test, *P<0.05) or xenon (Ba, t-test, *P<0.05), the expression of MEGF10 of the astrocytes has a significant decrease compared with the $A\beta_{1-42}$ treated only.*

AAV-MEGF10 siRNA knocked down the MEGF10 expression in dentate gyrus region of hippocampus

At last, I used the AAV type 9 to deliver the MEGF10 siRNA to the dentate gyrus region of the hippocampus to knock down the expression of MEGF10 (Fig. 17A). AAV-MEGF10 siRNA significantly reduced the protein level of MEGF10 in the hippocampus (Fig. 17B $P<0.05$) compared with the control virus.

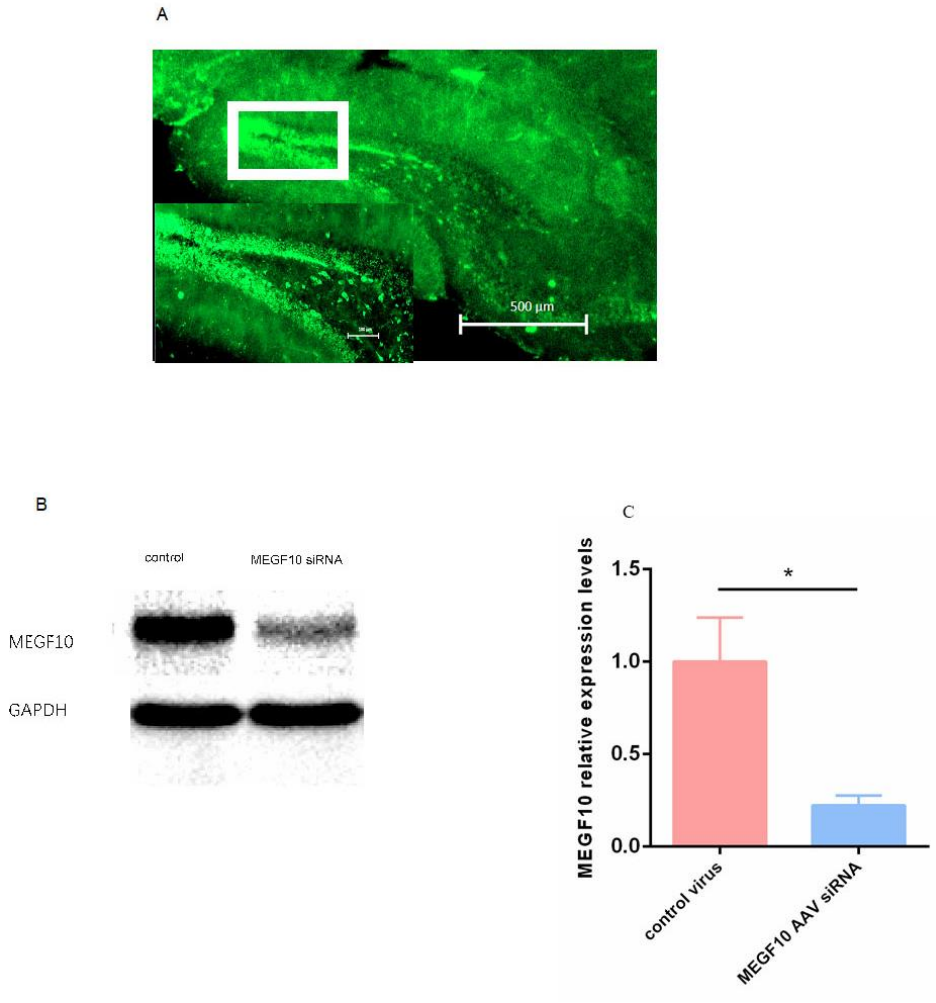

Fig 17: *AAV-MEGF10 siRNA knocked down the MEGF10 expression in dentate gyrus region of hippocampus. 17A the images showing the expression of enhanced GFP in dentate gyrus, indicative of neurons infected by the control virus or AAV-siRNA MEGF10. 17B the western blot membrane of the AAV injected brain slices. 17C it reveals that compared with the control virus, the AAV-siRNA MEGF10 significantly reduced the expression level of MEGF10 in hippocampi. T-test, *P<0.05.*

AAV-induced knock-down of MEGF10 reduced the pre- (synaptophysin) and postsynaptic (PSD95) marker inside astrocytes

Subsequently, I analyzed the pre–and postsynaptic marker inside the astrocytes of the dentate gyrus. The results showed that the pre- and postsynaptic elements inside the astrocytes were reduced in amount after MEGF10 gene knock down. (Fig. 18 pre: $P<0.05$; post: $P<0.05$)

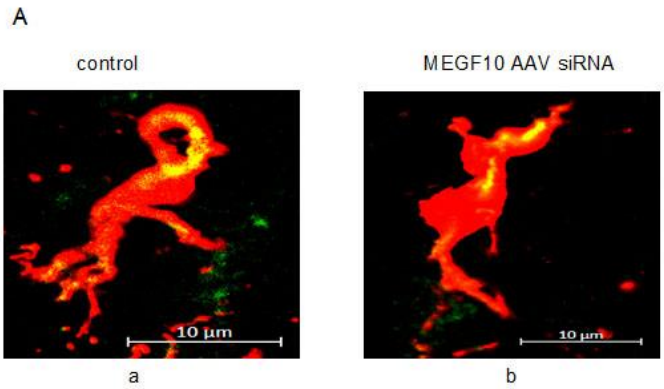

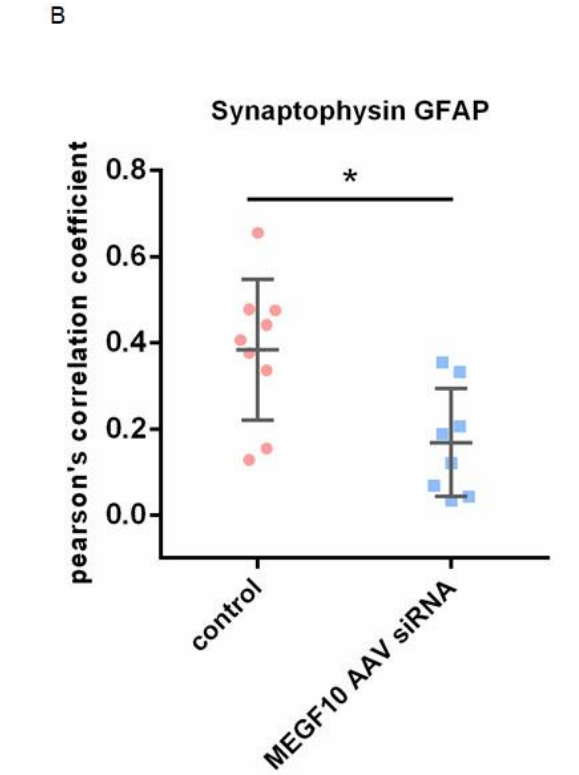

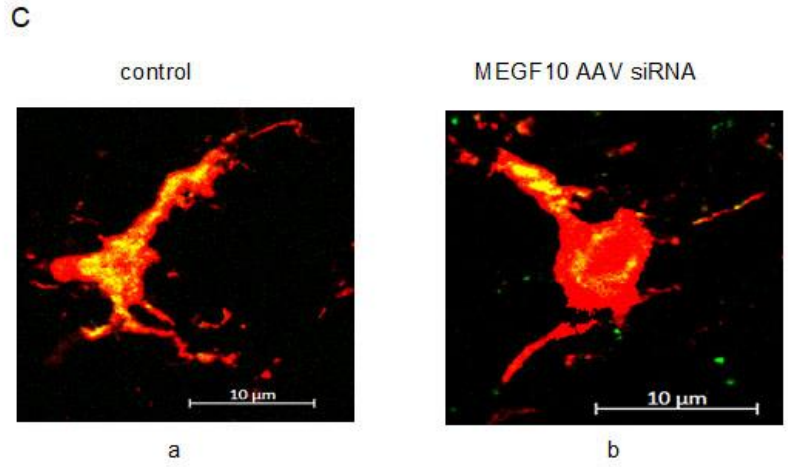

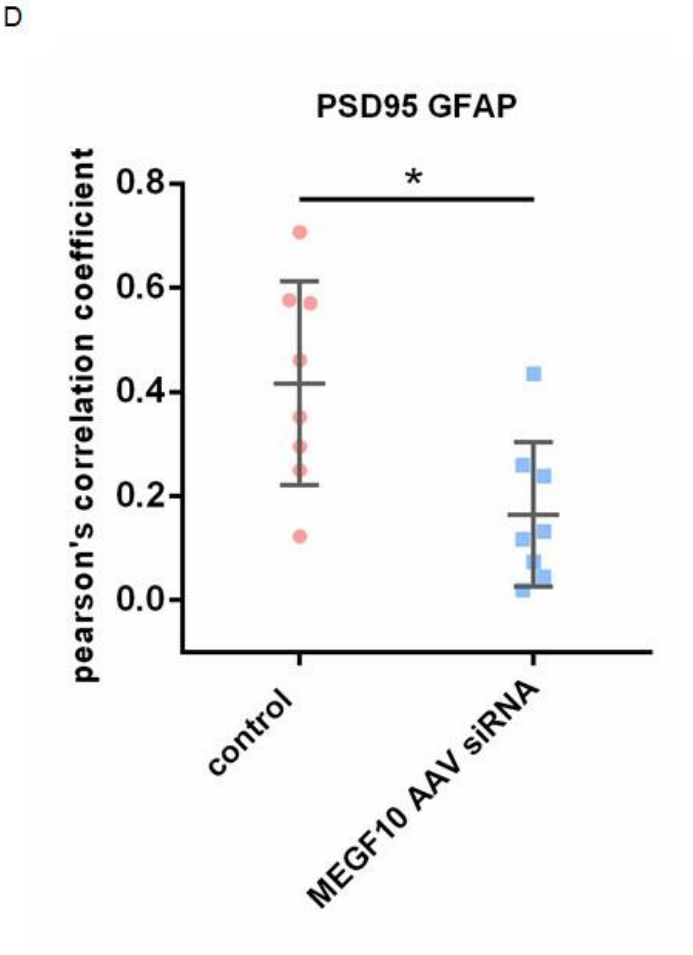

Fig 18: *AAV-induced knock-down of MEGF10 reduced the pre- (synaptophysin) and postsynaptic (PSD95) marker inside astrocytes. 18A the red is astrocyte, and the green is synaptophysin, the yellow dots inside the astrocytes are the by astrocytes engulfed presynaptic element. Compared with the control virus (Aa), in the AAV-siRNA*

*MEGF10 infected hippocampus (Ab), there are statistical less (18B) presynaptic elements engulfed by astrocytes. T-test, *P<0.05. 18C the red is astrocyte, and the green signal is PSD95, the yellow dots inside the astrocytes refer to the postsynaptic elements inside the astrocytes. Same as the presynaptic elements, there are statistical less (18D) postsynaptic elements engulfed by astrocytes in the AAV-siRNA MEGF10 infected hippocampus (18C a, b). T-test, *P<0.05.*

IV Discussion

Part i the effect of isoflurane and xenon on synapse loss through MEGF10 pathway

In this part of study, I applied 1% isoflurane and 65% xenon to brain slices and cultured astrocytes. The results showed that both isoflurane and xenon could decrease the dendritic spine density in dentate gyrus, but the reduction caused by xenon reversed after 60 min's xenon washout. I also observed that both isoflurane and xenon could reduce the expression of MEGF10 on the in-vitro cultured astrocytes. Even though neither isoflurane nor xenon affected physiological synapse engulfment significantly, in xenon treated slices presynaptic material inside astrocytes was tendencially attenuated.

The dendritic spines density of the brain slices decreased after 90-min gassing using 1% isoflurane. In clinic, the cognitive decline has been commonly observed after removing the anaesthetic. To resemble the clinical situation and investigate whether this reduction is persistent, the dendritic spines were also analyzed after 90min's isoflurane removal. The results showed that 90-min recovery could not reverse the reduction of dendritic spines density. Consistent with this study, it has been reported that isoflurane reduced the dendritic spines density in cultured hippocampal neurons[98]. However, one study observed that 1.5% isoflurane increased the dendritic spine density in the rat medial prefrontal cortex[93]. The discrepancy may be explained by the fact that

I studied the dentate gyrus of the hippocampus and used a lower dosage of isoflurane. However, based on previous literatures and results in the present study, it cannot be completely confirmed whether isoflurane could reduce the dendritic spines density persistently, because a 90-min of total recovery from an anesthetic might be not long enough. Nevertheless, the results of this study revealed that 1%isoflurane could decrease the dendritic spines density after 90-min recovery from isoflurane.

This study also demonstrated that xenon could reduce the dendritic spines density reversibly after 60-min's recovery from xenon. Although limited study investigated the direct interaction between xenon and spine density, the finding that xenon reduced the dendritic spine density was in line with one previous study that xenon attenuated the hippocampal LTP[75], suggesting that xenon could influence the hippocampal synaptic plasticity. In addition, this study demonstrated that, in contrast to isoflurane, the reduction of spine density mediated by xenon recovered after 60 min removal of the anesthetic. A few reasons were discussed as follows: the first of all, xenon and isoflurane have different mechanisms [54, 56, 64, 65]. Isoflurane can bind to GABA, glutamate and glycine receptors, while xenon is a NMDA, AMPA receptors antagonist. However, the NMDA receptor antagonism of xenon was reported very weak[65], which might be the reason of xenon's shorter effect on dendritic spines. Secondly, （0.37mM in aCSF=1.3-1.4MAC） and 65% xenon (1.9mM in aCSF= 0.4 MAC for mouse) were employed for mouse, respectively. The dose of isoflurane in this experiment was more two-fold of xenon. Therefore, the effect of isoflurane on the

dendritic spines was more intensive than xenon. Thirdly, since the regular time window for one operation is 90-min, thus1% isoflurane was employed for a period of 90-min. By contrast, as a very expensive anesthetic, xenon is not widely used in the clinic. Due to the lower blood gas partition coefficient, 0.115 as reported[99], the induction time and wake up time of xenon was shorter than isoflurane, whose blood gas partition coefficient is reported as 0.59[100], which means a shorter anesthetic time. In order to be consistent with the clinical application, xenon was employed with a duration of 60-min in this study. Different exposure times might also explain why the decrease in dendritic spines induced by xenon could be reversed.

Both anesthetics decreased the dendritic spine density, suggesting that less formation and/or more clearance of spines may occur after being treated with isoflurane and xenon. According to the mechanisms of isoflurane and xenon, isoflurane can enhance the GABA receptor function and attenuate the glutamate receptors' activity, while xenon can antagonise the NMDA, AMPA and kainate receptors. Both anesthetics could induce the reduction of synaptic activity[101, 102]. In this study, I investigated whether mainly spine elimination and not formation has been involved in this reduction. The western blot results showed that both isoflurane and xenon could down-regulate the expression of MEGF10 on the in-vitro cultured astrocytes. According to the phagocytic effect of MEGF10, the fact that isoflurane and xenon down-regulated the expression of MEGF10 on the astrocytes presumably revealed that the engulfment of synapses by astrocytes was inhibited. To verify this, the immunofluorescence was

performed, after gassing the brain slices with isoflurane and xenon as mentioned before. After analyzing the colocalization of GFAP and pre-or postsynaptic marker, the results showed that neither 1% isoflurane nor 65% xenon could change the engulfment of synapses by astrocytes significantly. 65%xenon decreased the presynaptic elements inside the astrocytes in amount marginally, whereas no change in the post-synaptic elements was observed. This is in line with the observation that xenon did not affect DSD.

Several reasons may explain this: First, one previous study suggested that the DSD changed immediately after the subject was anesthetized[98]. However, the results of this study showed that the expression of MEGF10 didn't change simultaneously as dendritic spine changed, suggesting that there weren't more spines cleaned by astrocytes. As the dynamic modification of dendritic spines concludes the formation and elimination[103], it may be plausible to speculate that this reduction was regulated by less formation. The isoflurane or xenon affected the new formation of dendritic spines via other unknown pathways, which was also consistent with the study that isoflurane affected the synaptogenesis in cortex[93]. In 2007, Ultanir et al. reported that NMDA receptors play a critical role in the dendritic spines density in the developing cortex[104]. Block the NR1subunit of NMDA receptor will induce the decrease in dendritic spines density[104]. Xenon is a glycine-site NMDA receptor antagonist, which may explain why xenon could decrease the dendritic spines density. The formation and elimination of the dendritic spines are supposed to have a dynamic balance in the healthy brain, thus less

formation is always accompanied with the reduction of elimination in the neurocircuit[105]. After the recovery from anesthetics, I observed a down-regulation of MEGF10 in astrocytes, which might induce the less clearance of synapses by astrocytes[46]. However, the number of synapses in astrocytes was not reduced, which might be because it takes longer time from the down-regulation of the phagocytic receptor to the reduction of the engulfment of synapses. The result that xenon reduced the pre-synaptic elements inside the astrocytes marginally supported this hypothesis to a certain extent. A further study with a longer period of observation is required to explain more about this in future. However, this experiment cannot be performed at this moment, because the in-vitro cultured brain slices could not stay active for more than 90-min, and a large number of cells in the in vitro cultured brain slices were dead or amorphognosia. Second, the brain is a complex network. The neurons, astrocytes, microglia and the other cell types have close connection and interaction. One phenomenon occurs in this circuit is the consequence of the interaction of different types of cells[106]. As the scavenger in the CNS, microglia can also participate in the clearance of dendritic spines[51, 107, 108]. Microglia-induced pruning of spines is dependent on the receptors CX3CR1 and CR3, which are microglia specific in the brain[51].The absence of CR3 and CX3CR1 would lead to the elevation of spine density in the adult mice brain[51]. However, whether microglia and astrocyte contribute equally to the synapse elimination or which one plays a more important role remains unknown.

Consequently, the interaction of different types of cells may lead to the decrease in the spine density.

This part simulated how isoflurane and xenon affect the synapse elimination through the MEGF10 pathway when the brain has no $A\beta_{1\text{-}42}$ aggregation. The results demonstrate that there might be a regulatory mechanism in the healthy brain slices. When less formation of dendritic spines was induced by isoflurane or xenon, the phagocytic receptor MEGF10 was down-regulated. These findings may reveal the mechanism underlying the lower incidence of POCD among the young and healthy people, although further study with a longer observation after anaesthesia is required to transfer this in-vitro experiment to clinic in future.

Part ii isoflurane and xenon reverse the effect of Aβ1-42 on the dendritic spine density through MEGF10 pathway

Over the past decades, amyloid-beta aggregation has been regarded as the earliest detectable change in the brain of AD patients [109]. Previous studies demonstrated that the soluble Aβ oligomers is associated with the memory loss [91, 109]. $A\beta_{1-42}$ oligomers could lead to the synapse degeneration and inhibit synaptic plasticity, particularly in the hippocampus[110-112]. The reduction of synaptic density plays an important role at staging dementia due to AD [19, 36, 113].

The results of the present study revealed that: 1) $A\beta_{1-42}$ could induce a reduction of dendritic spines density in the dentate gyrus region of the hippocampus, and elevate pre- and postsynaptic marker inside astrocytes; 2) the combined application with either isoflurane or xenon could reverse the decrease in dendritic spine density and the elevation of pre- and postsynaptic marker inside astrocytes caused by $A\beta_{1-42}$; 3) in the presence of $A\beta_{1-42,}$ both isoflurane and xenon inhibited MEGF10 expression in astrocytes; and 4) AAV-induced knock-down of MEGF10 reduced the pre- (synaptophysin) and postsynaptic (PSD95) marker inside astrocytes.

$A\beta_{1-42}$ reduced dendritic spines density in DG region, which was consistent with the previous studies in hippocampal pyramidal neurons[114] and in hippocampal CA1 region[21]. $A\beta_{1-42}$ decreased the dendritic spines density in the dentate gyrus region, indicating $A\beta_{1-42}$ decreased the excitatory synaptic inputs and induced the loss of synaptic contacts. In accordance with previous literatures[14, 21], this study also

demonstrated that $A\beta_{1-42}$ has synaptic toxic effects. In addition, LTP has been reported to be associated with the new formation of synapses[115], and previous reports revealed that $A\beta_{1-42}$ might inhibit LTP in the hippocampus[21, 116]. Together with previous literature, the findings in this study indicate that $A\beta_{1-42}$ might reduce the formation of new synapses.

There is no complete conclusion upon whether volatile anesthetics could be involved in the pathogenesis of postoperative cognitive dysfunction, whereas one previous study observed that isoflurane promotes cognitive impairment in the aged rodents perhaps by triggering the pathogenesis of AD[117]. Xenon has been regarded as neuroprotective [72]. However, it is still unknow whether people went under xenon anesthesia could have any different incidence in POCD compared with any other inhalation anesthetics[79]. As a major finding, this study demonstrated that both isoflurane and xenon could reverse the effect of $A\beta_{1-42}$ on the synaptic spine density and synapses elimination by astrocytes. I found that isoflurane and xenon showed similar effect on the reversal of $A\beta_{1-42}$. Both anesthetics reduce neuronal excitability which might counteract, e.g. overstimulation of NMDA receptors. In fact, it has been shown that $A\beta_{1-42}$ elevates NMDA receptor activity thereby increasing neuronal Ca^{2+}-influx[118, 119]. Both isoflurane and xenon reduce the overstimulation of NMDA receptors caused by $A\beta_{1-42}$ [55, 64], which was consistent with the previous report that NMDA antagonist reserved the synaptotoxic effect of $A\beta_{1-42}$ on LTP and dendritic spines density[21]. It has been reported that the underlying neurotoxic effects caused by an increase in

intracellular $A\beta_{1-42}$ lay in a rapid enhancement of AMPA receptor-mediated synaptic transmission[120]. Thus, the two anesthetics could bind to AMPA receptors, supporting that both anesthetics may reverse the effect of $A\beta_{1-42}$. $A\beta_{1-42}$ could down regulate GABA receptors, but isoflurane enhances the performance of GABA receptor [55, 121], which might be one potential mechanism underlying the reversal effects of isoflurane.

The formation and clearance of the spines are supposed to be in dynamic balance in the physiological process [30]. The reversal observed in this study could be a consequence of further more formation or less clearance. The results of the colocalization showed that isoflurane and xenon inhibited the phagocytosis of synapses in the presence of $A\beta_{1-42}$, indicating that less clearance might be one reason for the higher density of dendritic spines.

As a transmembrane protein existing on the surface of macrophages, astrocytes, and neuron[50], MEGF10 is responsible for astrocyte-dependent synapses elimination[46]. Applying the isoflurane or xenon to the pre-incubated with $A\beta_{1-42}$ in-vitro cultured astrocytes, the expression of MEGF10 in astrocytes was down-regulated, implying that the astrocytes-dependent elimination of the synapses was inhibited. Previous literatures reported that GABA and glutamate receptors are also expressed on astrocytes[122-124], implying that isoflurane and xenon can interact with those receptors on astrocytes directly. The astrocytic GABA receptor may be involved in extracellular ion homeostasis and pH regulation while functional glutamate receptors expressed on astrocytes can modulate other channels and receptors of the same cell[125, 126]. In addition,

AMPA receptors are involved in the modulation of gene expression[126]. Those may provide a potential explanation why isoflurane and xenon could influence the expression of MEGF10. However, the underlying mechanism still needs further investigation.

The number of synapses inside the astrocytes reduced as the down-regulation of MEGF10 expression using the AAV-siRNA, suggesting that this phagocytosis was dependent of MEGF10. These results suggest that isoflurane and xenon could reverse the $A\beta_{1-42}$-induced enhancement of synaptic elimination presumably through MEGF10 down-regulation.

Previous studies reported that isoflurane was proved to be neurotoxic[61, 127-129], while xenon was well established as a neuroprotective agent[68, 72]. Those two anesthetics have different mechanisms[56, 64, 74]. However, I did not observe a different effect of those two agents on the MEGF10 dependent synapses elimination in the presence of $A\beta_{1-42}$.

The interactions of isoflurane, xenon, and $A\beta_{1-42}$ on the dynamic properties of synapses might have implications for AD patients. However, it requires further study to reveal whether this reversal effect is beneficial or not. First, I only manifested the clearance of synapses by astrocytes via MEGF10 pathway without doing the research of the formation. Applying isoflurane and xenon might induce the new formation of dendritic spines, which needs to be verified by further study. Second, previous studies revealed that the MEGF10 expressed on the surface of astrocytes recognized the “eat me signal” C1q on the silent synapses[28,50]. Unsilencing and less pruning of those silent

synapses have been implicated in neurodevelopmental disorders[27]. MEGF10 is involved in the refinement of the neural circuit[52]. Less MEGF10 could result in the less clearance of silent synapses, leaving more silent synapses existing in the brain. However, it requires further study to testify which kind of synapses are involved in this phagocytosis. To detect whether this reversal is beneficial or not, a behavioral test is required in the subsequent study.

This study has some limitations which cannot be resolved perfectly right now due to the limitation of the experiment condition and the duration of the funding. Nevertheless, the results still provide a new thought to reveal the mechanism underlying the POCD, and the potential relationship between POCD and AD.

V Conclusion and outlook

Understanding the pathogenesis of POCD, and the potential relationship between POCD and AD is vital to avoid this age-dependent perioperative disorder and also helps understand the pathogenesis of AD. In addition, it should be explored whether anesthetics could trigger Aß pathophysiology in clinic, which will thereby enable the anesthesiologists to select a more suitable anesthetic for the AD patients or cognitively normal elderly adults with substantial amyloid plaques in the brain. In this study, I investigated the how isoflurane and xenon affect synapse loss in absence and presence of $A\beta_{1\text{-}42}$ respectively. Overall, my results provide a meaningful basis for further investigating of the basic mechanism of POCD and AD.

In the first part of this study, the effect of isoflurane and xenon on the density of dendritic spines was studied. Both isoflurane and xenon could decrease the dendritic spines density, whereas the reduction induced by xenon reversed after a certain time window. The delaying down-regulation of MEGF10 expression after the change of dendritic spines was observed in this study. Whether these two phenomenons are relative, and how they interact with each other still remains to be investigated in future. Under the normal condition, the dynamic balance of spines could keep balance after being exposed to xenon by the decrease in MEGF10 after 60min's recovery from xenon. Although I did not observe the same spine density reversal after isoflurane, the same delaying down-regulation of MEGF10 was still observed, suggesting that there could also be a trend to be balanced after a longer time's recovery.

In the second part of this study, the neurotoxic effect of $A\beta_{1-42}$ and the interaction of isoflurane/xenon and $A\beta_{1-42}$ were investigated. $A\beta_{1-42}$ induces the reduction of dendritic spines density, both isoflurane and xenon could reverse this down-regulation. The MEGF10 expression was down-regulated as long as fewer synapses were detected inside the astrocytes after exposure to those two anesthetics. These results demonstrated that isoflurane and xenon reverse the effect of $A\beta_{1-42}$ on the dendritic spines density presumably through MEGF10 pathway.

Nowadays, researchers worldwide have been committed to investigate the pathogenesis of POCD to address this perioperative disorder. Anesthesiologists are also trying to find the optimal anaesthetics and improve the method of anesthesia to avoid POCD. The potential relationship between POCD and AD are arousing increasing attention. Based on the results of this study, although I could not give a complete conclusion whether this reversal was beneficial or not, a new potential evidence was provided that xenon was neuroprotective while isoflurane might induce POCD, both of the two anesthetics could not trigger the $A\beta$ pathogenesis. This could also provide new evidence for the anesthesiologists to adopt a suitable method of anesthesia according to the age, or more precise, according to whether the patients have amyloid aggregation in the brain.

There are still a lot of questions to be addressed regarding to the influence of anesthesia upon elderly patients. Hopefully, we can address it via collaboration from different researchers all over the world in future.

VI Acknowledge

Over the past 3 years, I spent a wonderful time in Germany, particularly in Munich. I definitely learned more than what I wrote in this thesis. As soon as arrived in Munich, it did take me a while to get used to the new life in a new place, such as how to buy food, make local friends etc. I experienced different culture and enjoyed the great atmosphere here. I will treasure all of this in my whole life.

During my study in TUM, I received a lot of kind help from my colleagues and friends. Here I would like sincerely to appreciate them.

First of all, I would like to thank my supervisor Prof. Gerhard Rammes for giving me this opportunity to work in Experimental Anesthesiology, guiding and supporting the details work. His academic experience and thoughtful ideas always help me proceed in my project. As well as supervising my study, Gerhard also helped me a lot to get used to the new living and working place in Munich.

Meanwhile, I would like to thank all my lovely colleagues in Experimental Anesthesiology for their kind help in the daily work. Andi, Nina, Carolin, Tanja, Claudia, Xingxing, Catherina, Franzi and all of you other guys.

I acknowledge China scholarship council for financial support of my study and life in Munich.

I acknowledge Prof. Jochen Herms of German Center for Neurodegenerative Diseases for sharing their confocal microscopy to me, and also Dr. Kaichuan Zhu and the other colleagues in DZNE for their kind help.

I thank my husband Dr. Tengfei Guo and my parents for support and care in my daily life.

At last, thank you so much, my little boy. I feel so grateful that you choose me to be your mum. Last several months, it’s you to company me every moment. We share our happiness and sadness, success and failure. Every time when I feel upset or stressful, it’s your movement to give me courage and cheer me up. You and me, we together complete this thesis. Love you, my boy.

谨以此论文，送给我的儿子，郭慕时。

VII Reference

1. Alzheimer's, A., *2019 Alzheimer's disease facts and figures.* Alzheimers Dement, 2019. **15**(3): p. 321-387.
2. Tarawneh, R. and D.M. Holtzman, *The clinical problem of symptomatic Alzheimer disease and mild cognitive impairment.* Cold Spring Harb Perspect Med, 2012. **2**(5): p. a006148.
3. Selkoe, D.J., *Alzheimer's disease: genes, proteins, and therapy.* Physiol Rev, 2001. **81**(2): p. 741-66.
4. Goldman, J.S., S.E. Hahn, J.W. Catania, S. LaRusse-Eckert, M.B. Butson, M. Rumbaugh, M.N. Strecker, J.S. Roberts, W. Burke, R. Mayeux, T. Bird, G. American College of Medical, and C. the National Society of Genetic, *Genetic counseling and testing for Alzheimer disease: joint practice guidelines of the American College of Medical Genetics and the National Society of Genetic Counselors.* Genet Med, 2011. **13**(6): p. 597-605.
5. McKhann, G., D. Drachman, M. Folstein, R. Katzman, D. Price, and E.M. Stadlan, *Clinical diagnosis of Alzheimer's disease: report of the NINCDS-ADRDA Work Group under the auspices of Department of Health and Human Services Task Force on Alzheimer's Disease.* Neurology, 1984. **34**(7): p. 939-44.
6. McKhann, G.M., D.S. Knopman, H. Chertkow, B.T. Hyman, C.R. Jack, Jr., C.H. Kawas, W.E. Klunk, W.J. Koroshetz, J.J. Manly, R. Mayeux, R.C. Mohs, J.C. Morris, M.N. Rossor, P. Scheltens, M.C. Carrillo, B. Thies, S. Weintraub, and C.H. Phelps, *The diagnosis of dementia due to Alzheimer's disease: recommendations from the National Institute on Aging-Alzheimer's Association workgroups on diagnostic guidelines for Alzheimer's disease.* Alzheimers Dement, 2011. **7**(3): p. 263-9.
7. Irizarry, M.C., *Biomarkers of Alzheimer disease in plasma.* NeuroRx, 2004. **1**(2): p. 226-34.
8. Anoop, A., P.K. Singh, R.S. Jacob, and S.K. Maji, *CSF Biomarkers for Alzheimer's Disease Diagnosis.* Int J Alzheimers Dis, 2010. **2010**.
9. Binder, L.I., A.L. Guillozet-Bongaarts, F. Garcia-Sierra, and R.W. Berry, *Tau, tangles, and Alzheimer's disease.* Biochim Biophys Acta, 2005. **1739**(2-3): p. 216-23.
10. Haass, C. and D.J. Selkoe, *Soluble protein oligomers in neurodegeneration: lessons from the Alzheimer's amyloid beta-peptide.* Nat Rev Mol Cell Biol, 2007. **8**(2): p. 101-12.
11. Smith, M.A. and G. Perry, *The pathogenesis of Alzheimer disease: an alternative to the amyloid hypothesis.* J Neuropathol Exp Neurol, 1997. **56**(2): p. 217.

12. Mucke, L. and D.J. Selkoe, *Neurotoxicity of amyloid beta-protein: synaptic and network dysfunction.* Cold Spring Harb Perspect Med, 2012. **2**(7): p. a006338.
13. Barghorn, S., V. Nimmrich, A. Striebinger, C. Krantz, P. Keller, B. Janson, M. Bahr, M. Schmidt, R.S. Bitner, J. Harlan, E. Barlow, U. Ebert, and H. Hillen, *Globular amyloid beta-peptide oligomer - a homogenous and stable neuropathological protein in Alzheimer's disease.* J Neurochem, 2005. **95**(3): p. 834-47.
14. Ferreira, S.T. and W.L. Klein, *The Abeta oligomer hypothesis for synapse failure and memory loss in Alzheimer's disease.* Neurobiol Learn Mem, 2011. **96**(4): p. 529-43.
15. Xia, W., *Brain amyloid beta protein and memory disruption in Alzheimer's disease.* Neuropsychiatr Dis Treat, 2010. **6**: p. 605-11.
16. Spies, P.E., M.M. Verbeek, T. van Groen, and J.A. Claassen, *Reviewing reasons for the decreased CSF Abeta42 concentration in Alzheimer disease.* Front Biosci (Landmark Ed), 2012. **17**: p. 2024-34.
17. Citron, M., D. Westaway, W. Xia, G. Carlson, T. Diehl, G. Levesque, K. Johnson-Wood, M. Lee, P. Seubert, A. Davis, D. Kholodenko, R. Motter, R. Sherrington, B. Perry, H. Yao, R. Strome, I. Lieberburg, J. Rommens, S. Kim, D. Schenk, P. Fraser, P. St George Hyslop, and D.J. Selkoe, *Mutant presenilins of Alzheimer's disease increase production of 42-residue amyloid beta-protein in both transfected cells and transgenic mice.* Nat Med, 1997. **3**(1): p. 67-72.
18. Masliah, E., L. Crews, and L. Hansen, *Synaptic remodeling during aging and in Alzheimer's disease.* J Alzheimers Dis, 2006. **9**(3 Suppl): p. 91-9.
19. Selkoe, D.J., *Alzheimer's disease is a synaptic failure.* Science, 2002. **298**(5594): p. 789-91.
20. Terry, R.D., E. Masliah, D.P. Salmon, N. Butters, R. DeTeresa, R. Hill, L.A. Hansen, and R. Katzman, *Physical basis of cognitive alterations in Alzheimer's disease: synapse loss is the major correlate of cognitive impairment.* Ann Neurol, 1991. **30**(4): p. 572-80.
21. Rammes, G., F. Seeser, K. Mattusch, K. Zhu, L. Haas, M. Kummer, M. Heneka, J. Herms, and C.G. Parsons, *The NMDA receptor antagonist Radiprodil reverses the synaptotoxic effects of different amyloid-beta (Abeta) species on long-term potentiation (LTP).* Neuropharmacology, 2018. **140**: p. 184-192.
22. Izzo, N.J., A. Staniszewski, L. To, M. Fa, A.F. Teich, F. Saeed, H. Wostein, T. Walko, 3rd, A. Vaswani, M. Wardius, Z. Syed, J. Ravenscroft, K. Mozzoni, C. Silky, C. Rehak, R. Yurko, P. Finn, G. Look, G. Rishton, H. Safferstein, M. Miller, C. Johanson, E. Stopa, M. Windisch, B. Hutter-Paier, M. Shamloo, O. Arancio, H. LeVine, 3rd, and S.M. Catalano, *Alzheimer's therapeutics targeting amyloid beta 1-42 oligomers I: Abeta 42 oligomer binding to*

specific neuronal receptors is displaced by drug candidates that improve cognitive deficits. PLoS One, 2014. **9**(11): p. e111898.
23. Mayford, M., S.A. Siegelbaum, and E.R. Kandel, *Synapses and memory storage.* Cold Spring Harb Perspect Biol, 2012. **4**(6).
24. Atwood, H.L. and J.M. Wojtowicz, *Silent synapses in neural plasticity: current evidence.* Learn Mem, 1999. **6**(6): p. 542-71.
25. Favaro, P.D., X. Huang, L. Hosang, S. Stodieck, L. Cui, Y.Z. Liu, K.A. Engelhardt, F. Schmitz, Y. Dong, S. Lowel, and O.M. Schluter, *An opposing function of paralogs in balancing developmental synapse maturation.* PLoS Biol, 2018. **16**(12): p. e2006838.
26. Kerchner, G.A. and R.A. Nicoll, *Silent synapses and the emergence of a postsynaptic mechanism for LTP.* Nat Rev Neurosci, 2008. **9**(11): p. 813-25.
27. Hanse, E., H. Seth, and I. Riebe, *AMPA-silent synapses in brain development and pathology.* Nat Rev Neurosci, 2013. **14**(12): p. 839-50.
28. Bailey, C.H., E.R. Kandel, and K.M. Harris, *Structural Components of Synaptic Plasticity and Memory Consolidation.* Cold Spring Harb Perspect Biol, 2015. **7**(7): p. a021758.
29. Pham, E., L. Crews, K. Ubhi, L. Hansen, A. Adame, A. Cartier, D. Salmon, D. Galasko, S. Michael, J.N. Savas, J.R. Yates, C. Glabe, and E. Masliah, *Progressive accumulation of amyloid-beta oligomers in Alzheimer's disease and in amyloid precursor protein transgenic mice is accompanied by selective alterations in synaptic scaffold proteins.* FEBS J, 2010. **277**(14): p. 3051-67.
30. Nimchinsky, E.A., B.L. Sabatini, and K. Svoboda, *Structure and function of dendritic spines.* Annu Rev Physiol, 2002. **64**: p. 313-53.
31. Bosch, M. and Y. Hayashi, *Structural plasticity of dendritic spines.* Curr Opin Neurobiol, 2012. **22**(3): p. 383-8.
32. Knobloch, M. and I.M. Mansuy, *Dendritic spine loss and synaptic alterations in Alzheimer's disease.* Mol Neurobiol, 2008. **37**(1): p. 73-82.
33. Anand, K.S. and V. Dhikav, *Hippocampus in health and disease: An overview.* Ann Indian Acad Neurol, 2012. **15**(4): p. 239-46.
34. Mu, Y. and F.H. Gage, *Adult hippocampal neurogenesis and its role in Alzheimer's disease.* Mol Neurodegener, 2011. **6**: p. 85.
35. Scheff, S.W., D.A. Price, F.A. Schmitt, and E.J. Mufson, *Hippocampal synaptic loss in early Alzheimer's disease and mild cognitive impairment.* Neurobiol Aging, 2006. **27**(10): p. 1372-84.
36. Hamos, J.E., L.J. DeGennaro, and D.A. Drachman, *Synaptic loss in Alzheimer's disease and other dementias.* Neurology, 1989. **39**(3): p. 355-61.
37. Bertoni-Freddari, C., P. Fattoretti, T. Casoli, W. Meier-Ruge, and J. Ulrich, *Morphological adaptive response of the synaptic junctional zones in the human dentate gyrus during aging and Alzheimer's disease.* Brain Res, 1990. **517**(1-2): p. 69-75.

38. Morris, R.G., *Elements of a neurobiological theory of hippocampal function: the role of synaptic plasticity, synaptic tagging and schemas.* Eur J Neurosci, 2006. **23**(11): p. 2829-46.
39. Einstein, G., R. Buranosky, and B.J. Crain, *Dendritic pathology of granule cells in Alzheimer's disease is unrelated to neuritic plaques.* J Neurosci, 1994. **14**(8): p. 5077-88.
40. Williams, R.S. and S. Matthysse, *Age-related changes in Down syndrome brain and the cellular pathology of Alzheimer disease.* Prog Brain Res, 1986. **70**: p. 49-67.
41. Tatebayashi, Y., *[The dentate gyrus neurogenesis: a common therapeutic target for Alzheimer disease and senile depression?].* Seishin Shinkeigaku Zasshi, 2003. **105**(4): p. 398-404.
42. Sofroniew, M.V. and H.V. Vinters, *Astrocytes: biology and pathology.* Acta Neuropathol, 2010. **119**(1): p. 7-35.
43. Allen, N.J., *Astrocyte regulation of synaptic behavior.* Annu Rev Cell Dev Biol, 2014. **30**: p. 439-63.
44. Liddelow, S. and B. Barres, *SnapShot: Astrocytes in Health and Disease.* Cell, 2015. **162**(5): p. 1170-1170 e1.
45. Tasdemir-Yilmaz, O.E. and M.R. Freeman, *Astrocytes engage unique molecular programs to engulf pruned neuronal debris from distinct subsets of neurons.* Genes Dev, 2014. **28**(1): p. 20-33.
46. Chung, W.S., L.E. Clarke, G.X. Wang, B.K. Stafford, A. Sher, C. Chakraborty, J. Joung, L.C. Foo, A. Thompson, C. Chen, S.J. Smith, and B.A. Barres, *Astrocytes mediate synapse elimination through MEGF10 and MERTK pathways.* Nature, 2013. **504**(7480): p. 394-400.
47. Ziegenfuss, J.S., R. Biswas, M.A. Avery, K. Hong, A.E. Sheehan, Y.G. Yeung, E.R. Stanley, and M.R. Freeman, *Draper-dependent glial phagocytic activity is mediated by Src and Syk family kinase signalling.* Nature, 2008. **453**(7197): p. 935-9.
48. MacDonald, J.M., M.G. Beach, E. Porpiglia, A.E. Sheehan, R.J. Watts, and M.R. Freeman, *The Drosophila cell corpse engulfment receptor Draper mediates glial clearance of severed axons.* Neuron, 2006. **50**(6): p. 869-81.
49. Zhou, Z., E. Hartwieg, and H.R. Horvitz, *CED-1 is a transmembrane receptor that mediates cell corpse engulfment in C. elegans.* Cell, 2001. **104**(1): p. 43-56.
50. Iram, T., Z. Ramirez-Ortiz, M.H. Byrne, U.A. Coleman, N.D. Kingery, T.K. Means, D. Frenkel, and J. El Khoury, *Megf10 Is a Receptor for C1Q That Mediates Clearance of Apoptotic Cells by Astrocytes.* J Neurosci, 2016. **36**(19): p. 5185-92.
51. Chung, W.S., C.A. Welsh, B.A. Barres, and B. Stevens, *Do glia drive synaptic and cognitive impairment in disease?* Nat Neurosci, 2015. **18**(11): p. 1539-1545.

52. Chung, W.S., N.J. Allen, and C. Eroglu, *Astrocytes Control Synapse Formation, Function, and Elimination.* Cold Spring Harb Perspect Biol, 2015. **7**(9): p. a020370.
53. Singh, T.D., S.Y. Park, J.S. Bae, Y. Yun, Y.C. Bae, R.W. Park, and I.S. Kim, *MEGF10 functions as a receptor for the uptake of amyloid-beta.* FEBS Lett, 2010. **584**(18): p. 3936-42.
54. Jones, M.V., P.A. Brooks, and N.L. Harrison, *Enhancement of gamma-aminobutyric acid-activated Cl- currents in cultured rat hippocampal neurones by three volatile anaesthetics.* J Physiol, 1992. **449**: p. 279-93.
55. Lin, L.H., L.L. Chen, J.A. Zirrolli, and R.A. Harris, *General anesthetics potentiate gamma-aminobutyric acid actions on gamma-aminobutyric acidA receptors expressed by Xenopus oocytes: lack of involvement of intracellular calcium.* J Pharmacol Exp Ther, 1992. **263**(2): p. 569-78.
56. Jenkins, A., N.P. Franks, and W.R. Lieb, *Effects of temperature and volatile anesthetics on GABA(A) receptors.* Anesthesiology, 1999. **90**(2): p. 484-91.
57. Krasowski, M.D. and N.L. Harrison, *The actions of ether, alcohol and alkane general anaesthetics on GABAA and glycine receptors and the effects of TM2 and TM3 mutations.* Br J Pharmacol, 2000. **129**(4): p. 731-43.
58. Qiao, Y., H. Feng, T. Zhao, H. Yan, H. Zhang, and X. Zhao, *Postoperative cognitive dysfunction after inhalational anesthesia in elderly patients undergoing major surgery: the influence of anesthetic technique, cerebral injury and systemic inflammation.* BMC Anesthesiol, 2015. **15**: p. 154.
59. Arora, S.S., J.L. Gooch, and P.S. Garcia, *Postoperative cognitive dysfunction, Alzheimer's disease, and anesthesia.* Int J Neurosci, 2014. **124**(4): p. 236-42.
60. Lewis, M.C., I. Nevo, M.A. Paniagua, A. Ben-Ari, E. Pretto, S. Eisdorfer, E. Davidson, I. Matot, and C. Eisdorfer, *Uncomplicated general anesthesia in the elderly results in cognitive decline: does cognitive decline predict morbidity and mortality?* Med Hypotheses, 2007. **68**(3): p. 484-92.
61. Lin, D. and Z. Zuo, *Isoflurane induces hippocampal cell injury and cognitive impairments in adult rats.* Neuropharmacology, 2011. **61**(8): p. 1354-9.
62. Mandal, P.K. and J.W. Pettegrew, *Abeta peptide interactions with isoflurane, propofol, thiopental and combined thiopental with halothane: a NMR study.* Biochim Biophys Acta, 2008. **1778**(11): p. 2633-9.
63. Kuehn, B.M., *Anesthesia-Alzheimer disease link probed.* JAMA, 2007. **297**(16): p. 1760.
64. Weigt, H.U., K.J. Fohr, M. Georgieff, E.M. Georgieff, U. Senftleben, and O. Adolph, *Xenon blocks AMPA and NMDA receptor channels by different mechanisms.* Acta Neurobiol Exp (Wars), 2009. **69**(4): p. 429-40.
65. Haseneder, R., S. Kratzer, E. Kochs, D. Hofelmann, Y. Auberson, M. Eder, and G. Rammes, *The xenon-mediated antagonism against the NMDA receptor is non-selective for receptors containing either NR2A or NR2B subunits in the mouse amygdala.* Eur J Pharmacol, 2009. **619**(1-3): p. 33-7.

66. Haseneder, R., S. Kratzer, E. Kochs, V.S. Eckle, W. Zieglgansberger, and G. Rammes, *Xenon reduces N-methyl-D-aspartate and alpha-amino-3-hydroxy-5-methyl-4-isoxazolepropionic acid receptor-mediated synaptic transmission in the amygdala.* Anesthesiology, 2008. **109**(6): p. 998-1006.
67. Dinse, A., K.J. Fohr, M. Georgieff, C. Beyer, A. Bulling, and H.U. Weigt, *Xenon reduces glutamate-, AMPA-, and kainate-induced membrane currents in cortical neurones.* Br J Anaesth, 2005. **94**(4): p. 479-85.
68. Ma, D., S. Wilhelm, M. Maze, and N.P. Franks, *Neuroprotective and neurotoxic properties of the 'inert' gas, xenon.* Br J Anaesth, 2002. **89**(5): p. 739-46.
69. Winkler, D.A., A. Thornton, G. Farjot, and I. Katz, *The diverse biological properties of the chemically inert noble gases.* Pharmacol Ther, 2016. **160**: p. 44-64.
70. Banks, P., N.P. Franks, and R. Dickinson, *Competitive inhibition at the glycine site of the N-methyl-D-aspartate receptor mediates xenon neuroprotection against hypoxia-ischemia.* Anesthesiology, 2010. **112**(3): p. 614-22.
71. Liu, L.T., Y. Xu, and P. Tang, *Mechanistic insights into xenon inhibition of NMDA receptors from MD simulations.* J Phys Chem B, 2010. **114**(27): p. 9010-6.
72. Lavaur, J., M. Lemaire, J. Pype, D. Le Nogue, E.C. Hirsch, and P.P. Michel, *Neuroprotective and neurorestorative potential of xenon.* Cell Death Dis, 2016. **7**: p. e2182.
73. Bein, B., J. Hocker, and J. Scholz, *[Xenon--the ideal anaesthetic agent?].* Anasthesiol Intensivmed Notfallmed Schmerzther, 2007. **42**(11): p. 784-91.
74. Baskar, N. and J.D. Hunter, *Xenon as an anaesthetic gas.* Br J Hosp Med (Lond), 2006. **67**(12): p. 658-61.
75. Kratzer, S., C. Mattusch, E. Kochs, M. Eder, R. Haseneder, and G. Rammes, *Xenon attenuates hippocampal long-term potentiation by diminishing synaptic and extrasynaptic N-methyl-D-aspartate receptor currents.* Anesthesiology, 2012. **116**(3): p. 673-82.
76. Granger, A.J. and R.A. Nicoll, *Expression mechanisms underlying long-term potentiation: a postsynaptic view, 10 years on.* Philos Trans R Soc Lond B Biol Sci, 2014. **369**(1633): p. 20130136.
77. *NQF-Endorsed Measures for Surgical Procedures, 2015-2017.* 2017.
78. Turrentine, F.E., H. Wang, V.B. Simpson, and R.S. Jones, *Surgical risk factors, morbidity, and mortality in elderly patients.* J Am Coll Surg, 2006. **203**(6): p. 865-77.
79. Rundshagen, I., *Postoperative cognitive dysfunction.* Dtsch Arztebl Int, 2014. **111**(8): p. 119-25.

80. Steinmetz, J., K.B. Christensen, T. Lund, N. Lohse, L.S. Rasmussen, and I. Group, *Long-term consequences of postoperative cognitive dysfunction.* Anesthesiology, 2009. **110**(3): p. 548-55.
81. Newman, S., J. Stygall, S. Hirani, S. Shaefi, and M. Maze, *Postoperative cognitive dysfunction after noncardiac surgery: a systematic review.* Anesthesiology, 2007. **106**(3): p. 572-90.
82. Rasmussen, L.S., *Postoperative cognitive dysfunction: incidence and prevention.* Best Pract Res Clin Anaesthesiol, 2006. **20**(2): p. 315-30.
83. Krenk, L., L.S. Rasmussen, and H. Kehlet, *New insights into the pathophysiology of postoperative cognitive dysfunction.* Acta Anaesthesiol Scand, 2010. **54**(8): p. 951-6.
84. Yardeni, I.Z., B. Beilin, E. Mayburd, Y. Levinson, and H. Bessler, *The effect of perioperative intravenous lidocaine on postoperative pain and immune function.* Anesth Analg, 2009. **109**(5): p. 1464-9.
85. Watkins, L.R., L.E. Goehler, J. Relton, M.T. Brewer, and S.F. Maier, *Mechanisms of tumor necrosis factor-alpha (TNF-alpha) hyperalgesia.* Brain Res, 1995. **692**(1-2): p. 244-50.
86. Ramaiah, R. and A.M. Lam, *Postoperative cognitive dysfunction in the elderly.* Anesthesiol Clin, 2009. **27**(3): p. 485-96, table of contents.
87. Kline, R.P., E. Pirraglia, H. Cheng, S. De Santi, Y. Li, M. Haile, M.J. de Leon, A. Bekker, and I. Alzheimer's Disease Neuroimaging, *Surgery and brain atrophy in cognitively normal elderly subjects and subjects diagnosed with mild cognitive impairment.* Anesthesiology, 2012. **116**(3): p. 603-12.
88. Papon, M.A., R.A. Whittington, N.B. El-Khoury, and E. Planel, *Alzheimer's disease and anesthesia.* Front Neurosci, 2011. **4**: p. 272.
89. Evered, L., B. Silbert, D.A. Scott, D. Ames, P. Maruff, and K. Blennow, *Cerebrospinal Fluid Biomarker for Alzheimer Disease Predicts Postoperative Cognitive Dysfunction.* Anesthesiology, 2016. **124**(2): p. 353-61.
90. Xie, Z., S. McAuliffe, C.A. Swain, S.A. Ward, C.A. Crosby, H. Zheng, J. Sherman, Y. Dong, Y. Zhang, N. Sunder, D. Burke, K.J. Washicosky, R.E. Tanzi, and E.R. Marcantonio, *Cerebrospinal fluid abeta to tau ratio and postoperative cognitive change.* Ann Surg, 2013. **258**(2): p. 364-9.
91. Klein, W.L., G.A. Krafft, and C.E. Finch, *Targeting small Abeta oligomers: the solution to an Alzheimer's disease conundrum?* Trends Neurosci, 2001. **24**(4): p. 219-24.
92. Isik, B., *Postoperative cognitive dysfunction and Alzheimer disease.* Turk J Med Sci, 2015. **45**(5): p. 1015-9.
93. Briner, A., M. De Roo, A. Dayer, D. Muller, W. Habre, and L. Vutskits, *Volatile anesthetics rapidly increase dendritic spine density in the rat medial prefrontal cortex during synaptogenesis.* Anesthesiology, 2010. **112**(3): p. 546-56.

94. Kaech, S., H. Brinkhaus, and A. Matus, *Volatile anesthetics block actin-based motility in dendritic spines.* Proc Natl Acad Sci U S A, 1999. **96**(18): p. 10433-7.
95. Cetin, A., S. Komai, M. Eliava, P.H. Seeburg, and P. Osten, *Stereotaxic gene delivery in the rodent brain.* Nat Protoc, 2006. **1**(6): p. 3166-73.
96. *Image Lab Software User Guide - Bio-Rad.*
97. Liu, O. and B.D. Grant, *Basolateral Endocytic Recycling Requires RAB-10 and AMPH-1 Mediated Recruitment of RAB-5 GAP TBC-2 to Endosomes.* PLoS Genet, 2015. **11**(9): p. e1005514.
98. Platholi, J., K.F. Herold, H.C. Hemmings, Jr., and S. Halpain, *Isoflurane reversibly destabilizes hippocampal dendritic spines by an actin-dependent mechanism.* PLoS One, 2014. **9**(7): p. e102978.
99. Goto, T., K. Suwa, S. Uezono, F. Ichinose, M. Uchiyama, and S. Morita, *The blood-gas partition coefficient of xenon may be lower than generally accepted.* Br J Anaesth, 1998. **80**(2): p. 255-6.
100. Esper, T., M. Wehner, C.D. Meinecke, and H. Rueffert, *Blood/Gas partition coefficients for isoflurane, sevoflurane, and desflurane in a clinically relevant patient population.* Anesth Analg, 2015. **120**(1): p. 45-50.
101. Owens, D.F. and A.R. Kriegstein, *Is there more to GABA than synaptic inhibition?* Nat Rev Neurosci, 2002. **3**(9): p. 715-27.
102. Hoffmann, H., T. Gremme, H. Hatt, and K. Gottmann, *Synaptic activity-dependent developmental regulation of NMDA receptor subunit expression in cultured neocortical neurons.* J Neurochem, 2000. **75**(4): p. 1590-9.
103. Bhatt, D.H., S. Zhang, and W.B. Gan, *Dendritic spine dynamics.* Annu Rev Physiol, 2009. **71**: p. 261-82.
104. Ultanir, S.K., J.E. Kim, B.J. Hall, T. Deerinck, M. Ellisman, and A. Ghosh, *Regulation of spine morphology and spine density by NMDA receptor signaling in vivo.* Proc Natl Acad Sci U S A, 2007. **104**(49): p. 19553-8.
105. Stein, I.S. and K. Zito, *Dendritic Spine Elimination: Molecular Mechanisms and Implications.* Neuroscientist, 2018: p. 1073858418769644.
106. Halassa, M.M. and P.G. Haydon, *Integrated brain circuits: astrocytic networks modulate neuronal activity and behavior.* Annu Rev Physiol, 2010. **72**: p. 335-55.
107. Jung, Y.J. and W.S. Chung, *Phagocytic Roles of Glial Cells in Healthy and Diseased Brains.* Biomol Ther (Seoul), 2018.
108. Ransohoff, R.M. and V.H. Perry, *Microglial physiology: unique stimuli, specialized responses.* Annu Rev Immunol, 2009. **27**: p. 119-45.
109. Hardy, J. and D.J. Selkoe, *The amyloid hypothesis of Alzheimer's disease: progress and problems on the road to therapeutics.* Science, 2002. **297**(5580): p. 353-6.
110. Gong, Y., L. Chang, K.L. Viola, P.N. Lacor, M.P. Lambert, C.E. Finch, G.A. Krafft, and W.L. Klein, *Alzheimer's disease-affected brain: presence of*

oligomeric A beta ligands (ADDLs) suggests a molecular basis for reversible memory loss. Proc Natl Acad Sci U S A, 2003. **100**(18): p. 10417-22.
111. Lacor, P.N., M.C. Buniel, L. Chang, S.J. Fernandez, Y. Gong, K.L. Viola, M.P. Lambert, P.T. Velasco, E.H. Bigio, C.E. Finch, G.A. Krafft, and W.L. Klein, *Synaptic targeting by Alzheimer's-related amyloid beta oligomers.* J Neurosci, 2004. **24**(45): p. 10191-200.
112. Townsend, M., G.M. Shankar, T. Mehta, D.M. Walsh, and D.J. Selkoe, *Effects of secreted oligomers of amyloid beta-protein on hippocampal synaptic plasticity: a potent role for trimers.* J Physiol, 2006. **572**(Pt 2): p. 477-92.
113. Hatanpaa, K., K.R. Isaacs, T. Shirao, D.R. Brady, and S.I. Rapoport, *Loss of proteins regulating synaptic plasticity in normal aging of the human brain and in Alzheimer disease.* J Neuropathol Exp Neurol, 1999. **58**(6): p. 637-43.
114. Shrestha, B.R., O.V. Vitolo, P. Joshi, T. Lordkipanidze, M. Shelanski, and A. Dunaevsky, *Amyloid beta peptide adversely affects spine number and motility in hippocampal neurons.* Mol Cell Neurosci, 2006. **33**(3): p. 274-82.
115. Toni, N., P.A. Buchs, I. Nikonenko, C.R. Bron, and D. Muller, *LTP promotes formation of multiple spine synapses between a single axon terminal and a dendrite.* Nature, 1999. **402**(6760): p. 421-5.
116. Walsh, D.M., I. Klyubin, J.V. Fadeeva, W.K. Cullen, R. Anwyl, M.S. Wolfe, M.J. Rowan, and D.J. Selkoe, *Naturally secreted oligomers of amyloid beta protein potently inhibit hippocampal long-term potentiation in vivo.* Nature, 2002. **416**(6880): p. 535-9.
117. Zhang, S., X. Hu, W. Guan, L. Luan, B. Li, Q. Tang, and H. Fan, *Isoflurane anesthesia promotes cognitive impairment by inducing expression of beta-amyloid protein-related factors in the hippocampus of aged rats.* PLoS One, 2017. **12**(4): p. e0175654.
118. Rammes, G., A. Gravius, M. Ruitenberg, N. Wegener, C. Chambon, K. Sroka-Saidi, R. Jeggo, L. Staniaszek, D. Spanswick, E. O'Hare, P. Palmer, E.M. Kim, W. Bywalez, V. Egger, and C.G. Parsons, *MRZ-99030 - A novel modulator of Abeta aggregation: II - Reversal of Abeta oligomer-induced deficits in long-term potentiation (LTP) and cognitive performance in rats and mice.* Neuropharmacology, 2015. **92**: p. 170-82.
119. Birnbaum, J.H., J. Bali, L. Rajendran, R.M. Nitsch, and C. Tackenberg, *Calcium flux-independent NMDA receptor activity is required for Abeta oligomer-induced synaptic loss.* Cell Death Dis, 2015. **6**: p. e1791.
120. Whitcomb, D.J., E.L. Hogg, P. Regan, T. Piers, P. Narayan, G. Whitehead, B.L. Winters, D.H. Kim, E. Kim, P. St George-Hyslop, D. Klenerman, G.L. Collingridge, J. Jo, and K. Cho, *Intracellular oligomeric amyloid-beta rapidly regulates GluA1 subunit of AMPA receptor in the hippocampus.* Sci Rep, 2015. **5**: p. 10934.
121. Ulrich, D., *Amyloid-beta Impairs Synaptic Inhibition via GABA(A) Receptor Endocytosis.* J Neurosci, 2015. **35**(24): p. 9205-10.

122. Losi, G., L. Mariotti, and G. Carmignoto, *GABAergic interneuron to astrocyte signalling: a neglected form of cell communication in the brain.* Philos Trans R Soc Lond B Biol Sci, 2014. **369**(1654): p. 20130609.
123. Kirchhoff, F., *Analysis of Functional NMDA Receptors in Astrocytes.* Methods Mol Biol, 2017. **1677**: p. 241-251.
124. Fan, D., S.Y. Grooms, R.C. Araneda, A.B. Johnson, K. Dobrenis, J.A. Kessler, and R.S. Zukin, *AMPA receptor protein expression and function in astrocytes cultured from hippocampus.* J Neurosci Res, 1999. **57**(4): p. 557-71.
125. Hoft, S., S. Griemsmann, G. Seifert, and C. Steinhauser, *Heterogeneity in expression of functional ionotropic glutamate and GABA receptors in astrocytes across brain regions: insights from the thalamus.* Philos Trans R Soc Lond B Biol Sci, 2014. **369**(1654): p. 20130602.
126. Seifert, G. and C. Steinhauser, *Ionotropic glutamate receptors in astrocytes.* Prog Brain Res, 2001. **132**: p. 287-99.
127. Stratmann, G., J.W. Sall, L.D. May, J.S. Bell, K.R. Magnusson, V. Rau, K.H. Visrodia, R.S. Alvi, B. Ku, M.T. Lee, and R. Dai, *Isoflurane differentially affects neurogenesis and long-term neurocognitive function in 60-day-old and 7-day-old rats.* Anesthesiology, 2009. **110**(4): p. 834-48.
128. Lemkuil, B.P., B.P. Head, M.L. Pearn, H.H. Patel, J.C. Drummond, and P.M. Patel, *Isoflurane neurotoxicity is mediated by p75NTR-RhoA activation and actin depolymerization.* Anesthesiology, 2011. **114**(1): p. 49-57.
129. Xie, Z., Y. Dong, U. Maeda, P. Alfille, D.J. Culley, G. Crosby, and R.E. Tanzi, *The common inhalation anesthetic isoflurane induces apoptosis and increases amyloid beta protein levels.* Anesthesiology, 2006. **104**(5): p. 988-94.